CHALMERS

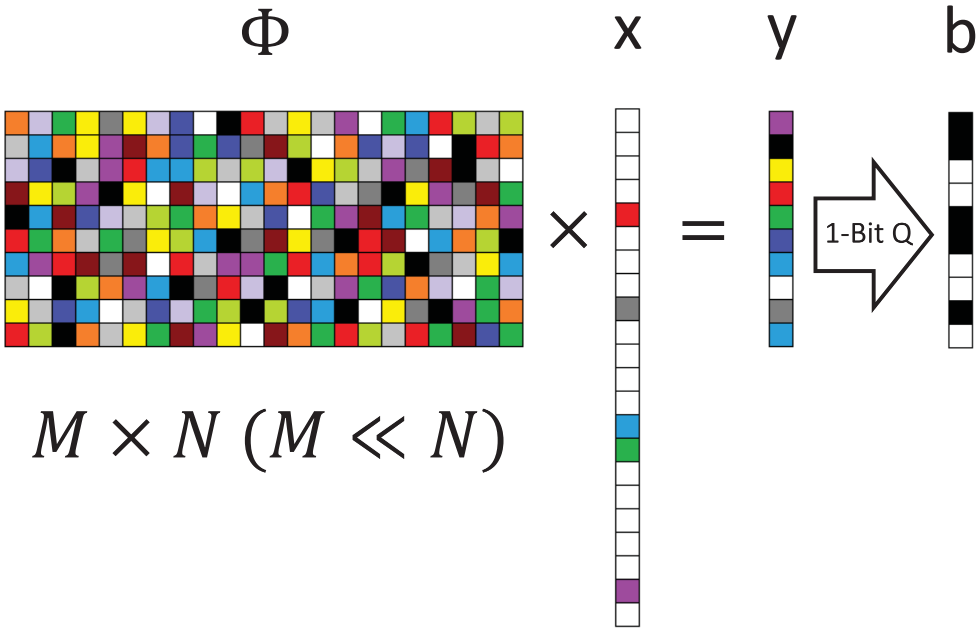

Recovery guarantee and reconstruction algorithms for 1-bit compressive sensing

Amin Movahed

Communication Systems and Information Theory
Department of Signals and Systems
CHALMERS UNIVERSITY OF TECHNOLOGY
Gothenburg, Sweden

EX030/2012

Thesis for the degree of Master of Science

Recovery guarantee and reconstruction algorithms for 1-bit compressive sensing

by

Amin Movahed

Department of Signals and Systems
Division of Communication systems and Information Theory
CHALMERS UNIVERSITY OF TECHNOLOGY

Gothenburg, Sweden 2012

Recovery guarantee and reconstruction algorithms for 1-bit compressive sensing

Amin Movahed

This thesis has been prepared using LaTeX.

EX030/2012.

Department of Signals and Systems
Division of Communication systems and Information Theory
Chalmers University of Technology
SE-412 96 Gothenburg, Sweden

email: Movahed@student.chalmers.se

Cover:
The big picture of 1-bit compressive sensing. Binary measurements vector $\mathbf{b}$ is obtained by 1-bit quantization of measurements vector $\mathbf{y}$ which is generated by compressive sensing (measurement matrix $\mathbf{\Phi} \in \mathbb{R}^{M\times N}$) over signal vector $\mathbf{x}$.

To my dear and loving family

Recovery guarantee and reconstruction algorithms for 1-bit compressive sensing

Amin Movahed
Department of Signals and Systems
Division of Communication Systems and Information Theory
Chalmers University of Technology

Abstract

Compressive sensing is an emerging method for signal acquisition in which the number of samples ensuring exact reconstruction of the signal to be acquired is far less than the one in the conventional Nyquist sampling approach. In compressive sensing, the signal is acquired by means of few linear non-adaptive measurements, and then reconstructed by finding the sparsest solution via an ℓ_1-minimization.

In the classic compressive sensing setup, each measurement outcome is described by a real value. In practice, for further processing and storage purposes, often the real-valued measurements need to be converted to finite-precision numbers. 1-bit compressive sensing refers to the extreme case where the quantizer is a simple sign comparator and each measurement is represented using one bit only, i.e., $+1$ or -1.

Several algorithms have been introduced in the literature for solving efficiently the reconstruction problem in the 1-bit compressive sensing setting, e.g., *renormalized fixed point iteration* (RFPI) and *binary iterative hard thresholding* (BIHT). However, these algorithms can not reconstruct the signal accurately when there is noise, i.e., bit flips, in the binary measurements. *Adaptive outlier pursuit* (AOP) is an algorithm which reconstructs the signal robustly against bit flips in the binary measurements. AOP requires the sparsity level of the signal to be reconstructed as an input. In many practical cases, however, the sparsity level of the signal is unknown and time variant.

In this thesis, we address reconstruction problem in 1-bit compressive sensing. We introduce a new algorithm for 1-bit compressive sensing which reconstructs the signal robustly from the noisy binary measurements. This new reconstruction algorithm does not require the sparsity level of the signal as an input. Therefore, our algorithm can be applied in the most practical scenarios in which the sparsity level of the signal is unknown.

Keywords: 1-bit quantization, compressive sensing, iterative algorithms, ℓ_1-minimization.

Acknowledgments

I am heartily thankful to my supervisor, Giuseppe Durisi, whose encouragement, guidance and support from the initial to the final level enabled me to develop an understanding of the subject.
Moreover, I would like to show my gratitude to my dear friend, Ashkan Panahi, from whom I learned many valuable things during this work.

Amin Movahed

Contents

List of Figures

List of Tables

Abbreviations, Acronyms and Notations

Abbreviations and Acronyms

AOP	adaptive outlier pursuit
AOP-ℓ_2	adaptive outlier pursuit using ℓ_2-norm minimization
AOP-f	adaptive outlier pursuit with sign flips
AOP-f-ℓ_2	adaptive outlier pursuit with sign flips using ℓ_2-norm minimization
BIHT	binary iterative hard thresholding
BIHT-ℓ_2	binary iterative hard thresholding using ℓ_2-norm minimization
BSC	binary symmetric channel
IHT	iterative hard thresholding
NARFPI	noise adaptive renormalized fixed point iteration
RFPI	renormalized fixed point iteration
RIP	restricted isometry property

Notations

$\|\cdot\|_0$	ℓ_0-norm (Number of non-zero elements)
$\|\cdot\|_1$	ℓ_1-norm
$\|\cdot\|_2$	ℓ_2-norm (Euclidean norm)
$\|\cdot\|_{\mathrm{F}}$	Frobenius-norm
$\odot$	element-wise product
$(\cdot)^-$	negative function
$\emptyset$	empty set
$\lvert T\rvert$	number of elements in set T
$\langle\cdot,\cdot\rangle$	inner product
$\backslash$	set minus
$\succeq$	element-wise inequality
$[\cdot]_i$	ith element of the argument
$\mathbf{b}$	binary measurements vector
$\tilde{\mathbf{b}}$	noisy binary measurements vector
$\mathbb{C}$	set of complex numbers
$\mathrm{diag}(\mathbf{b})$	a diagonal matrix whose diagonal is vector $\mathbf{b}$
$\mathbb{E}(\cdot)$	expected value of the argument
$\exp(\cdot)$	exponential function
$\mathbf{\Phi}$	measurement matrix
$\mathbf{\Phi}^\dagger$	conjugate transpose of $\mathbf{\Phi}$
$\mathbf{\Phi}^T$	transpose of $\mathbf{\Phi}$
$\mathbf{\Phi}^{-1}$	pseudo-inverse of $\mathbf{\Phi}$
$\mathbf{\Phi}_{[:,T]}$	a sub-matrix of $\mathbf{\Phi}$ spanned to columns of $\mathbf{\Phi}$ in set T

$\boldsymbol{\Phi}_{[V,:]}$	a sub-matrix of $\boldsymbol{\Phi}$ spanned to rows of $\boldsymbol{\Phi}$ in set V
$\phi_{i,:}$	the ith row of $\boldsymbol{\Phi}$
$\phi_{i,j}$	the element of $\boldsymbol{\Phi}$ in row i and column j
$\mathcal{H}_s(\cdot)$	a non-linear operator that keeps the s largest elements of the argument and set the other elements to zero
$\ker\{\boldsymbol{\Phi}\}$	null-space of matrix $\boldsymbol{\Phi}$
$\lambda_{\max}(\boldsymbol{\Phi})$	maximum eigenvalue of matrix $\boldsymbol{\Phi}$
$\lambda_{\min}(\boldsymbol{\Phi})$	minimum eigenvalue of matrix $\boldsymbol{\Phi}$
$\boldsymbol{\Lambda}$	a binary vector containing 0s and 1s
M	dimension of the measurements vector
N	dimension of the signal vector
$[N]$	set of numbers from 1 to N
$\mathcal{N}(\mu, \sigma^2)$	normal distribution with mean μ and variance σ^2
$\boldsymbol{\Omega}$	a binary vector containing -1s and 1s
$\mathcal{O}(\cdot)$	order of the argument
P_f	probability of sign flips
$\mathbb{P}(\cdot)$	probability of the argument
$\mathbb{R}$	set of real numbers
s	sparsity level of the signal
$\mathrm{Supp}(\mathbf{x})$	set of indices of non-zero elements in $\mathbf{x}$
$\mathrm{Sub}(c^2)$	sub-Gaussian distribution with constant c
$\mathrm{SSub}(c^2)$	strictly Sub-Gaussian distribution with constant c
$\sigma_{\max}(\boldsymbol{\Phi})$	maximum singular value of matrix $\boldsymbol{\Phi}$
$\sigma_{\min}(\boldsymbol{\Phi})$	minimum singular value of matrix $\boldsymbol{\Phi}$
$\mathrm{tr}(\boldsymbol{\Phi})$	trace of matrix $\boldsymbol{\Phi}$

T^c	complement of set T
$\mathbf{x}$	signal vector
$\hat{\mathbf{x}}$	estimation of signal vector
$\mathbf{x}^{[n]}$	vector $\mathbf{x}$ in nth iteration
$\mathbf{x}_T$	a vector containing elements of $\mathbf{x}$ spanned to the indices in set T
$\mathbf{y}$	measurements vector
$\tilde{\mathbf{y}}$	noisy measurements vector

Chapter 1

Introduction

1.1 Introduction to 1-bit compressive sensing

The Nyquist sampling theorem specifies that to avoid information loss when measuring a signal, one must sample it at least two times faster than the signal bandwidth [1]. In many applications, like digital image and video cameras, the Nyquist rate is so high that the samples need to be compressed before storage or transmission. Furthermore, increasing the sampling rate is very expensive and impractical in applications like medical image scanners, radars and high-speed analog-to-digital converters.

Compressive sensing provides a completely new approach to data acquisition by suggesting that it is possible to improve the traditional Nyquist limits of sampling theory [2]. Compressive sensing predicts that certain signals can be recovered from low rate measurements which are not sufficient according to Nyquist sampling theorem. Compressive sensing is based on the empirical observation that many types of signals or images can be well-approximated by a sparse expansion in terms of a suitable basis [3, 4]. For example, in digital imaging systems, sparse signals can be obtained by applying wavelet transformation over original captured images. In compressive sensing, each measurement is obtained through an inner product between the vector of the sparse signal and the vector containing measuring elements. Then, the sparse signal can be reconstructed from few number of these measurements via an ℓ_1-minimization. In recent years, compressive sensing has attracted considerable attention in many areas of applied mathematics, computer science, and electrical engineering.

There are two main research topics in compressive sensing. The first topic is about establishing mathematically rigorous recovery guarantees relating the signal dimension, the sparsity level of the signal and the number of measurements. The task of the second topic is to find algorithms that reconstruct the signals accurately from the measurements obtained by compressive sensing. E. Candès and T. Tao [5] showed that sparse signals can be reconstructed through an ℓ_1-minimization when the measurement system is satisfying *restricted isometry property*. There are various reconstruction algorithms for compressive sensing. We single out the paper by J. A. Tropp and S. J. Wright [6] in which various types of algorithms for sparse reconstruction from compressive sensing are explained.

In practice, the measured signal should pass through a quantizer, which is located between the measuring and the recovering layers, provides recognizable data for further storage or transmission [7]. The quantizer affects the signal reconstruction accuracy. Performance analysis of the effects of the quantization and the noise of the measurement on various data reconstruction methods in compressive sensing is an emerging research topic. In this work, we focus on the extreme class of quantizers that have only two quantization levels, i.e., each quantized value is characterized by only one bit. *1-bit compressive sensing* is the combination of compressive sensing with a 1-bit quantizer, which was first introduced by P. Boufounos and R. Baraniuk [8].

The main focus of this thesis is on the iterative reconstruction algorithms in 1-bit compressive sensing. As reconstruction solutions for 1-bit compressive sensing, two different iterative algorithms were introduced by P. Boufounos and R. Baraniuk [8] and L. Jacques et al. [9] for signal reconstruction in noiseless 1-bit compressive sensing. However, the reconstruction process becomes more challenging when there is noise in the quantized measurements. An iterative algorithm that is robust against noise in 1-bit compressive sensing has been proposed by M. Yan et al. [10]. This algorithm reconstructs the signal from the noisy binary measurements based on the following a priori information: 1) the sparsity level of the signal and 2) the amount of noise in the binary measurements.

1.2 The key contribution of the thesis

In many practical applications, the sparsity level of the signal is not known and, therefore, the algorithm proposed in [10] can not be fed by an exact input of the signal sparsity level. As the main contribution of this thesis, we propose an algorithm which works robustly against noise in 1-bit compressive sensing and does not need the sparsity level of the signal to be reconstructed as an input. Hence, this new algorithm can be applied in many practical scenarios in which the sparsity level of the signal is unknown and time-variant. Another contribution of this thesis is to review and put the theoretical results, relating reconstruction guarantees in compressive sensing and 1-bit compressive sensing, in a single framework.

1.3 The structure of the thesis

- **Chapter 2**: We start the first part of this chapter by defining the compressive sensing problem and the conditions in which linear measurements system in compressive sensing can guarantee a perfect signal reconstruction. In this thesis we mainly focus on iterative reconstruction algorithms, therefore, in the second part of this chapter, we introduce an iterative reconstruction algorithm for compressive sensing.

- **Chapter 3**: We define the 1-bit compressive sensing problem. We also explain the conditions guaranteeing reconstruction in 1-bit compressive sensing. Due to time constraints, we do not provide details of the proof of reconstruction guarantees in 1-bit compressive sensing. We also introduce some iterative reconstruction algorithms for 1-bit compressive sensing, e.g. BIHT, BIHT-ℓ_2 and RFPI, designed to work in the noiseless scenario.

- **Chapter 4**: In the first part, we model the binary noise in 1-bit compressive sensing. In the second part, we discuss reconstruction algorithms designed to perform robustly in the presence of the noise, e.g. AOP, AOP-ℓ_2, AOP-f and AOP-f-ℓ_2. In the third part, we propose our contribution which is a new reconstruction algorithm, NARFPI, that is robust against noise and does not need any a priori knowledge of the signal sparsity level.

- **Chapter 5**: We evaluate the algorithms through Matlab simulations. In the first part, we compare the performance of the iterative algorithms designed for noiseless case in the noiseless and the noisy scenarios. In the second part, we compare the performance of our new algorithm with the algorithms designed to work in the noisy scenario and in the case that sparsity level of the signal is unknown.

- **Chapter 6**: We summarize the results obtained from previous chapters and we discuss about possible future work to extend the proposed reconstruction algorithm.
- **Appendix A**: The theorems in Chapter 2 are proved in detail.
- **Appendix B**: We present a model for measurement noise to be used in Chapter 4.

Chapter 2

Compressive sensing

2.1 Recovery via ℓ_1-minimization

In this chapter, we introduce the compressive sensing problem and then we show the conditions in which the recovery for compressive sensing is guaranteed. In addition, we explain an iterative reconstruction algorithm for compressive sensing.

2.1.1 Sparse Recovery

Signal vector $\mathbf{x}$ is called s-sparse if no more than s of its elements have non-zero values, i.e., $\|\mathbf{x}\|_0 \leq s$. In compressive sensing, a s-sparse signal is measured through few non-adaptive linear measurements. In other words, let $\mathbf{x} \in \mathbb{C}^N$ be an N-dimensional vector that is s-sparse. $\mathbf{y} \in \mathbb{C}^M$, which is called *measurements vector*, is obtained by left multiplying $\mathbf{x}$ with the *measurement matrix* $\mathbf{\Phi} \in \mathbb{C}^{M \times N}$ according to

$$\mathbf{\Phi x} = \mathbf{y}. \tag{2.1}$$

We are interested in the case when the dimension of the measurements vector is less than the dimension of the signal, that is, $M \ll N$. Since $\mathbf{\Phi}$ is a fat matrix, by solving (2.1) for $\mathbf{x}$ we obtain infinitely many solutions. By imposing the additional requirement that $\mathbf{x}$ is s-sparse, the problem changes to searching for the sparsest solution of (2.1). Therefore, we need to solve the ℓ_0-minimization problem

$$\begin{aligned} \hat{\mathbf{x}} = \arg\min_{\mathbf{x}} \|\mathbf{x}\|_0 \\ \text{subject to } \mathbf{\Phi x} = \mathbf{y} \end{aligned} \tag{2.2}$$

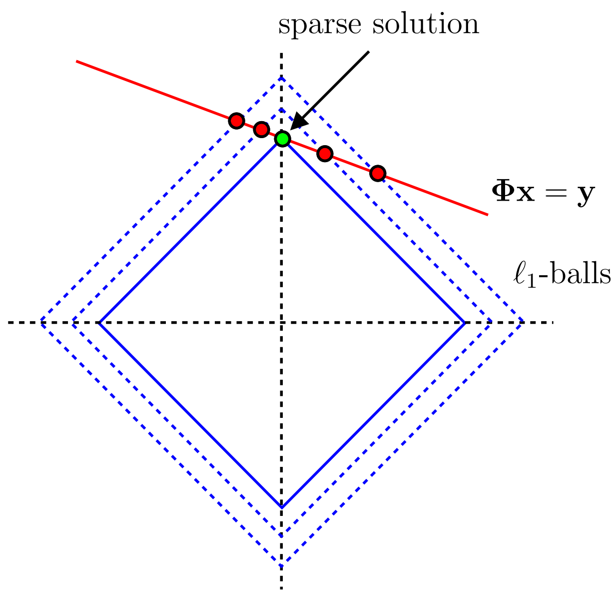

Figure 2.1: The intersection point between ℓ_1-ball and $\mathbf{\Phi x} = \mathbf{y}$ in 2-dimensional space.

where $\hat{\mathbf{x}}$ denotes estimation of $\mathbf{x}$. Unfortunately, (2.2) is an NP-hard problem [11] and is not easy to solve. One approach to solve (2.2) is to use convex relaxation. The ℓ_1-minimization problem

$$\begin{aligned} &\hat{\mathbf{x}} = \arg\min_{\mathbf{x}} \|\mathbf{x}\|_1 \\ &\text{subject to } \mathbf{\Phi x} = \mathbf{y} \end{aligned} \tag{2.3}$$

is a convex relaxation of (2.2) [12]. In Figure 2.1, the mechanism of solving (2.3) in 2-dimensional space is shown. In words, the intersection point between the smallest possible ℓ_1-ball and $\mathbf{\Phi x} = \mathbf{y}$ is the sparsest solution satisfying $\mathbf{\Phi x} = \mathbf{y}$. Note that the sparse $\hat{\mathbf{x}}$ in 2-dimensional space is a 2-dimensional vector with a zero in one of its two elements. (we selected the 2-dimensional space for the sake of simplicity, however, this mechanism holds for every N-dimensional space). Therefore, the problem of compressive sensing converts to solving (2.3).

2.1.2 Null space property and restricted isometry property

In order to make sure that through solving (2.3) we obtain a unique solution coinciding with the solution of (2.2), the measurement matrix $\mathbf{\Phi}$ should fulfil some requirements. First, we define *null space property* and show that in the case this property holds, the solution of ℓ_1-minimization is unique. Then, we define another property called *restricted isometry property* (RIP) and we show that RIP guarantees null space property.

Null space property

Definition 1. A matrix $\mathbf{\Phi} \in \mathbb{C}^{M \times N}$ satisfies the null space property of order s if for all $S \subset [N]$, $\mid S \mid= s$ we have that

$$\|\mathbf{v}_S\|_1 < \|\mathbf{v}_{S^c}\|_1 \text{ for all } \mathbf{v} \in \ker\{\mathbf{\Phi}\} \setminus \{0\} \tag{2.4}$$

where $[N] = \{1, 2, \ldots, N\}, \ker\{\mathbf{\Phi}\} = \{\mathbf{x} \in \mathbb{C}^N,\ \mathbf{\Phi}\mathbf{x} = 0\}$,$\mathbf{v}_S = (v_j)_{j \in S}$ *and* $S^c = [N] \setminus S$.

The next theorem shows the importance of null space property in compressive sensing reconstruction via ℓ_1-minimization.

Theorem 1 ([12, Theorem 2.3])**.** *Let* $\mathbf{\Phi} \in \mathbb{C}^{M \times N}$. *Every s-sparse vector* $\mathbf{x} \in \mathbb{C}^N$ *is the unique solution of ℓ_1-minimization problem* (2.3) *with* $\mathbf{\Phi}\mathbf{x} = \mathbf{y}$ *if and only if* $\mathbf{\Phi}$ *satisfies the null space property of order s.*

Theorem 1 is proved in Appendix A.1.

Restricted isometry property

Definition 2. For each $s = 1, 2, ...$ and for all s-sparse $\mathbf{x} \in \mathbb{C}^N$, we define δ_s to be the smallest scalar such that

$$(1 - \delta_s) \parallel \mathbf{x} \parallel_2^2 \leq \parallel \mathbf{\Phi}\mathbf{x} \parallel_2^2 \leq (1 + \delta_s) \parallel \mathbf{x} \parallel_2^2 \text{ for all } s\text{-sparse } \mathbf{x}\,. \tag{2.5}$$

Then, the matrix $\mathbf{\Phi}$ is said to satisfy the *restricted isometry property* (RIP) with *restricted isometry constant* δ_s.

The following theorem shows in which conditions on restricted isometry constant, null space property holds.

Theorem 2 ([12, Theorem 2.3])**.** *Let* $\mathbf{\Phi} \in \mathbb{C}^{M \times N}$ *has restricted isometry constant* $\delta_{2s} < 1/3$. *Then* $\mathbf{\Phi}$ *satisfies the null space property of order s.*

Theorem 2 is proved in Appendix A.2.

2.2 Random matrices and RIP

Up to here, we showed how the signal recovery through ℓ_1-minimization can be guaranteed by RIP. In this section, we explain which matrices are obeying this property and are suitable to be applied in compressive sensing.

2.2.1 Gaussian random matrices

Definition 3 ([13, Definition 2.1])**.** A standard real/complex Gaussian $M \times N$ matrix $\mathbf{\Phi}$ has i.i.d. real/complex zero-mean Gaussian entries with identical variance $\sigma^2 = 1/M$. The probability density function of a complex Gaussian matrix with i.i.d. zero-mean Gaussian entries with variance σ^2 is

$$\left(\pi\sigma^2\right)^{-MN} \exp\left[-\frac{\mathrm{tr}\left(\mathbf{\Phi}\mathbf{\Phi}^\dagger\right)}{\sigma^2}\right]. \tag{2.6}$$

Theorem 3 ([14])**.** *Let $\mathbf{\Phi} \in \mathbb{C}^{M\times N}$ be a random Gaussian matrix with zero-mean and $\sigma^2 = 1/M$. If*

$$M \geq \frac{4}{k^2} s \log\left(N/s\right) \tag{2.7}$$

$\mathbf{\Phi}$ satisfies RIP for $\delta_{2s} < 1/3$ with probability greater than

$$1 - 2\exp\left(2s\log\left(N/2s\right) - Mk^2/2\right) \tag{2.8}$$

for every $0 < k < 0.15 - \sqrt{2s/M}$.

Theorem 3 is proved in Appendix A.3. The main result of Theorem 3 is that any random Gaussian matrix, whose number of rows is (2.7), satisfies null space property with high probability and, therefore, $\mathbf{x}$ can be reconstructed accurately through solving (2.3).

2.2.2 Sub-Gaussian random matrices

In the following, we introduce sub-Gaussian matrices and we show in which conditions on this class of matrices RIP is satisfied.

Definition 4. A random variable X is called *sub-Gaussian* if there exists a constant $c > 0$ such that

$$\mathbb{E}\left(\exp\left(Xt\right)\right) \leq \exp\left(c^2t^2/2\right), \tag{2.9}$$

where $t \in \mathbb{R}$. We use the notation $X \sim \mathrm{Sub}\left(c^2\right)$ to denote that X satisfies (2.9).

Lemma 1 ([15, Lemma 1.2])**.** *If $X \sim \mathrm{Sub}\left(\mathrm{c}^2\right)$ then $\mathbb{E}\left(X\right) = 0$ and $\mathbb{E}\left(X^2\right) \leq c^2$.*

This lemma shows that if $X \sim \mathrm{Sub}\left(\mathrm{c}^2\right)$ then $\sigma^2 \leq c^2$ where σ^2 is the variance of X. In the case that $\sigma^2 = c^2$, we define more specific class of distributions.

Definition 5. If $X \sim \mathrm{Sub}\left(\sigma^2\right)$ where $\sigma^2 = \mathbb{E}\left(X^2\right)$ then X is called *strictly sub-Gaussian* and we use the notation $X \sim \mathrm{SSub}\left(\sigma^2\right)$.

Theorem 4 ([16, Theorem 7.3])**.** *Let $\mathbf{\Phi} \in \mathbb{C}^{M\times N}$ whose entries ϕ_{ij} are i.i.d. with $\phi_{ij} \sim \mathrm{SSub}\left(1/M\right)$ and $\delta_s \in (0,1)$. If*

$$M \geq \alpha s \log\left(N/s\right), \tag{2.10}$$

then $\mathbf{\Phi}$ satisfies RIP of order s with probability greater than $1-2e^{-\beta M}$, where α is arbitrary, $\beta = \delta_s^2/2\mu - \log\left(42e/\delta_s\right)/\alpha$ and $\mu = 2/(1-\log(2))$.

Theorem 4 is proved in Appendix A.4. Theorem 4 proves that any matrix whose elements are strictly sub-Gaussian fulfils RIP with restricted isometry constant δ_s when the number of rows is (2.10).

2.3 Iterative hard thresholding

In the previous sections, we discussed about the characteristic of the measuring matrix which guarantees the reconstruction. In this section and next chapters, we focus on the reconstruction algorithms. Throughout this work, we assume that $\mathbf{\Phi}$ is a real random Gaussian matrix. Gaussian random matrices are practically easy to generate and, therefore, no prior storage is needed. One natural variation of compressive sensing problem is to relax constraint in (2.2) and allow some error tolerance $\varepsilon \geq 0$ [6]. Therefore, we obtain

$$\begin{aligned} &\hat{\mathbf{x}} = \arg\min_{\mathbf{x}} \left\|\mathbf{x}\right\|_0 \\ &\text{subject to } \left\|\mathbf{y} - \mathbf{\Phi}\mathbf{x}\right\|_2 \leq \varepsilon \end{aligned} \tag{2.11}$$

The measurement error can be defined in different ways. In (2.11), the predicted measurement error is measured by euclidean norm. In the case that the sparsity level of $\mathbf{x}$, s, is known as a priori knowledge, the problem in (2.11) can be written as follows:

$$\begin{aligned} &\hat{\mathbf{x}} = \arg\min_{\mathbf{x}} \left\|\mathbf{y} - \mathbf{\Phi}\mathbf{x}\right\|_2 \\ &\text{subject to} \qquad \left\|\mathbf{x}\right\|_0 \leq s. \end{aligned} \tag{2.12}$$

The minimization (2.12) searches for the best approximation of $\mathbf{x}$ with the given maximum sparsity level s. In [17], an iterative algorithm called *iterative hard thresholding* (IHT) is introduced which solves (2.12) iteratively. IHT includes two steps. The first step consists of a gradient descent to reduce

Algorithm 1 IHT

1. **Inputs:** measurements vector $\mathbf{y}$, measurement matrix $\mathbf{\Phi}$, sparsity level of the signal s, descent step size τ, number of iterations t
2. **Initialization:** Initial estimate $\mathbf{x}^{[0]} = \mathbf{0}$
3. **Iteration:** For $n = 1, \ldots, t$
   (a) **Gradient descent:** $\mathbf{z}^{[n]} \leftarrow \mathbf{x}^{[n-1]} - \tau\mathbf{\Phi}^T \left(\mathbf{\Phi}\mathbf{x}^{[n-1]} - \mathbf{y}\right)$
   (b) **Projection onto "ℓ_0-ball":** $\mathbf{x}^{[n]} \leftarrow \mathcal{H}_s(\mathbf{z}^{[n]})$
4. **Output:** $\hat{\mathbf{x}} = \frac{\mathbf{x}^{[n]}}{\|\mathbf{x}^{[n]}\|_2}$

$\|\mathbf{y} - \mathbf{\Phi}\mathbf{x}\|_2$. The second step generates a sparse signal model by projecting the output of the step one onto the "ℓ_0-ball" by selecting the s largest elements in $\mathbf{x}$ obtained from the previous step. Therefore, each iteration step is as follows:

$$\mathbf{x}^{[n+1]} = \mathcal{H}_s(\mathbf{x}^{[n]} + \mathbf{\Phi}^T(\mathbf{y} - \mathbf{\Phi}\mathbf{x}^{[n]})) \tag{2.13}$$

where $\mathbf{x}^{[n]}$ denotes $\mathbf{x}$ in nth iteration, $\mathbf{x}^{[0]} = \mathbf{0}$ and $\mathcal{H}_s(\cdot)$ is a non-linear operator that keeps the s largest elements of the argument and set the other elements to zero. It is shown that when $\mathbf{\Phi}$ satisfies RIP the solution of (2.13) converges through iterations [18]. The steps of IHT are shown in detail in Algorithm 1.

The euclidean distance between the signal and its estimation, i.e., $\|\mathbf{x} - \hat{\mathbf{x}}\|_2$ is a measure of reconstruction quality. In Figure 2.2, the rate of successful signal reconstruction (i.e., $\|\mathbf{x} - \hat{\mathbf{x}}\|_2 < 10^{-5}$) via IHT among 4000 realizations is shown for different number of measurements M, where $N = 1000$, $s = 10$, $t = 200$ and $\mathbf{\Phi}$ is a Gaussian random matrix. As it is expected, when M tends to N ($M/N \to 1$), the rate of successful signal reconstruction converges to 100%. That is, when $M = N$ the linear equation system is not undetermined and definitely has a unique solution.

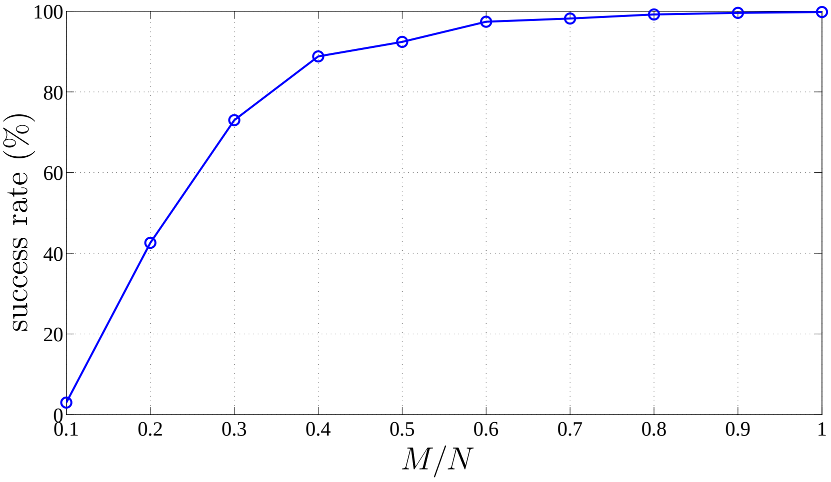

Figure 2.2: The rate of successful signal reconstruction via IHT

Chapter 3

1-bit compressive sensing

3.1 1-bit compressive sensing problem

In Chapter 2, we introduced the classic compressive sensing problem. This problem is based on the fact that measurements vector $\mathbf{y}$ has infinite bit precision. However, in practice measurements should be quantized for further storage and transmission. In the case the quantizer has only one bit, it is called 1-bit compressive sensing. That is, by sensing the signal through measuring matrix we obtain measurements vector and its 1-bit quantized version is called *binary measurements vector*. This binary vector is denoted by $\mathbf{b}$ and we have

$$\mathbf{b} = \operatorname{sign}\left(\mathbf{\Phi x}\right). \tag{3.1}$$

1-bit quantizer is a comparator to zero which is very fast and inexpensive hardware device. Therefore, it has many advantages in comparison to other types of quantizers in hardware implementation. As Boufounos et al. mentions [8], "1-bit quantizers do not suffer from dynamic range issues. If the analog side of the measurement system is properly implemented then the sign of the measurement remains valid even if the quantizer saturates".

3.2 1-bit compressive sensing reconstruction

Inspired by (2.3), the problem of 1-bit compressive sensing reconstruction can be written as

$$\begin{aligned} &\hat{\mathbf{x}} = \arg\min_{\mathbf{x}} \|\mathbf{x}\|_1 \\ &\text{subject to} \quad \operatorname{sign}(\mathbf{\Phi x}) = \mathbf{b}. \end{aligned} \tag{3.2}$$

That is, by replacing the constraint $\mathbf{\Phi x} = \mathbf{y}$ in (2.3) with $\text{sign}(\mathbf{\Phi x}) = \mathbf{b}$, we obtain (3.2). However, the optimization problem in (3.2) is not convex and, therefore, is not easy to solve. In [19], it is suggested that by applying $\|\mathbf{\Phi x}\|_1 = M$ as an extra constraint over (3.2), following convex optimization can be obtained

$$\begin{aligned} &\hat{\mathbf{x}} = \arg\min_{\mathbf{x}} \|\mathbf{x}\|_1 \\ &\text{subject to} \quad \text{sign}(\mathbf{\Phi x}) = \mathbf{b}. \\ &\text{and} \quad \|\mathbf{\Phi x}\|_1 = M. \end{aligned} \tag{3.3}$$

In fact, $\text{sign}(\mathbf{\Phi x}) = \mathbf{b}$ and $\|\mathbf{\Phi x}\|_1 = M$ can be combined and represented as one linear equation

$$\|\mathbf{\Phi x}\|_1 = \sum_{i=1}^{M} |\langle \phi_{i,:}, \mathbf{x} \rangle| = \sum_{i=1}^{M} [\mathbf{b}]_i \langle \phi_{i,:}, \mathbf{x} \rangle = M \tag{3.4}$$

where $[\cdot]_i$ denotes the ith element of the argument and $\phi_{i,:}$ denotes the ith row of $\mathbf{\Phi}$. Therefore, (3.3) is indeed a convex minimization program [19]. In addition, for the sake of simplicity and without loss of generality, both the original and the reconstructed signals are imposed to be on "ℓ_2-ball" with unite radius (energy normalization). Hence, constraint $\|\mathbf{x}\|_2 = 1$ is added to (3.3) and we have

$$\begin{aligned} &\hat{\mathbf{x}} = \arg\min_{\mathbf{x}} \|\mathbf{x}\|_1 \\ &\text{subject to} \quad \text{sign}(\mathbf{\Phi x}) = \mathbf{b} \\ &\text{and} \quad \|\mathbf{\Phi x}\|_1 = M, \quad \|\mathbf{x}\|_2 = 1. \end{aligned} \tag{3.5}$$

Theorem 5 ([19, Corollary 1.2])**.** *Let $\mathbf{\Phi}$ be an $M \times N$ random Gaussian matrix. Set*

$$\delta = C \left(\frac{s}{M} \log(2N/s) \log(2N/M + 2M/N) \right)^{1/5}. \tag{3.6}$$

Then for all s-sparse signals $\mathbf{x} \in \mathbb{R}^N$, with probability at least $1 - C\exp(-c\delta M)$, the solution $\hat{\mathbf{x}}$ of the convex minmization program (3.5) satisfies

$$\|\hat{\mathbf{x}} - \mathbf{x}\|_2 \leq \delta. \tag{3.7}$$

Here, C and c denote positive absolute constants and term $\|\hat{\mathbf{x}} - \mathbf{x}\|_2$ is a measure of the reconstruction quality. A useful conclusion of Theorem 5 can

Figure 3.1: 1-bit compressive sensing and reconstruction block diagram

be stated as follows:
An arbitrary accurate estimation of every s-sparse vector $\mathbf{x}$ can be achieved from M one-bit random measurements with order of $s\log^2(N/s)$. To be more precise $M \sim \delta^{-5} s \log^2(N/s)$ [19].

Due to time constraints, we do not prove Theorem 5 in this work. Theorem 5 has been proved in [19].

3.3 Iterative reconstruction algorithms for 1-bit compressive sensing

In this section, several iterative reconstruction algorithms for 1-bit compressive sensing are introduced. In Figure 3.1, the block diagrams of 1-bit compressive sensing and reconstruction part are shown. In this setup it is assumed that the binary measurements vector $\mathbf{b}$ is noiseless. We will investigate the noisy scenario in the next chapter.

3.3.1 BIHT

Binary iterative hard thresholding (BIHT) is a reconstruction algorithm first introduced in [9] and further investigated in [7]. BIHT is derived from IHT and tries to minimize $\|\mathbf{b} - \operatorname{sign}(\mathbf{\Phi x})\|_2$ over $\mathbf{x}$ where $\mathbf{b}$ and $\mathbf{\Phi}$ are given. Therefore, BIHT solves the following problem

$$\begin{aligned} \hat{\mathbf{x}} = \arg\min_{\mathbf{x}} &\|\mathbf{b} - \operatorname{sign}(\mathbf{\Phi x})\|_2 \\ \text{subject to} \quad &\|\mathbf{x}\|_0 \leq s, \ \|\mathbf{x}\|_2 = 1. \end{aligned} \tag{3.8}$$

It has been proved that minimization (3.8) is similar to [9, Lemma 5]

$$\begin{aligned} \hat{\mathbf{x}} = \arg\min_{\mathbf{x}} &\left\|(\mathbf{b} \odot \mathbf{\Phi x})^-\right\|_1 \\ \text{subject to} \quad &\|\mathbf{x}\|_0 \leq s, \ \|\mathbf{x}\|_2 = 1, \end{aligned} \tag{3.9}$$

where $\odot$ denotes the element-wise vector multiplication, i.e., $[\mathbf{u} \odot \mathbf{v}]_i = u_i v_i$ and $(\cdot)^-$denotes the negative function, i.e. $\left[(\mathbf{v})^-\right]_i = \begin{cases} -v_i & v_i \leq 0 \\ 0 & v_i > 0 \end{cases}$.

Algorithm 2 BIHT

1. **Inputs:** binary measurements vector $\mathbf{b} \in \{\pm 1\}^M$, measurement matrix $\boldsymbol{\Phi}$, sparsity level of the signal s, descent step size τ, number of iterations t

2. **Initialization:** Initial estimate $\mathbf{x}^{[0]} = \mathbf{0}$

3. **Iteration:** For $n = 1, \ldots, t$

   (a) **Gradient descent:** $\mathbf{z}^{[n]} \leftarrow \mathbf{x}^{[n-1]} - \tau \boldsymbol{\Phi}^T \left(\text{sign}\left(\boldsymbol{\Phi}\mathbf{x}^{[n-1]}\right) - \mathbf{b}\right)$

   (b) **Projection onto "ℓ_0-ball":** $\mathbf{x}^{[n]} \leftarrow \mathcal{H}_s(\mathbf{z}^{[n]})$

4. **Output:** $\hat{\mathbf{x}} = \frac{\mathbf{x}^{[n]}}{\left\|\mathbf{x}^{[n]}\right\|_2}$

In other words, when the signal is approximated perfectly we have $\mathbf{b} = \text{sign}(\boldsymbol{\Phi}\mathbf{x})$ and $[\mathbf{b} \odot \boldsymbol{\Phi}\mathbf{x}]_i > 0$ for all i. BIHT tries to minimize the summation of the absolute values of the negative elements in $\mathbf{b} \odot \boldsymbol{\Phi}\mathbf{x}$ iteratively. The iterative step of BIHT is

$$\mathbf{x}^{[n+1]} = \mathcal{H}_s(\mathbf{x}^{[n]} - \boldsymbol{\Phi}^T(\text{sign}(\boldsymbol{\Phi}\mathbf{x}^{[n]}) - \mathbf{b})). \tag{3.10}$$

In Algorithm 2, the steps of BIHT are shown in detail.

3.3.2 BIHT-ℓ_2

If ℓ_2-norm is applied in BIHT instead of ℓ_1-norm, we obtain BIHT-ℓ_2 which has been discussed in [7, 9, 20]. BIHT-ℓ_2 algorithm can be thought of as trying to solve:

$$\begin{aligned} &\hat{\mathbf{x}} = \arg\min_{\mathbf{x}} \left\| (\mathbf{b} \odot \mathbf{\Phi x})^- \right\|_2 \\ &\text{subject to} \quad \|\mathbf{x}\|_0 \leq s, \ \|\mathbf{x}\|_2 = 1. \end{aligned} \tag{3.11}$$

In fact, BIHT-ℓ_2 tries to minimize

$$\sum_{i \in V} \left([\mathbf{b} \odot \mathbf{\Phi x}]_i \right)^2, \tag{3.12}$$

where $\mathbf{x}$ is s-sparse and V is a set of indices in which $\mathbf{b} \odot \mathbf{\Phi x}$ is negative. In [9], it is shown that the solution of (3.11) can be obtained by simply iterating the following step:

$$\mathbf{x}^{[n+1]} = \mathcal{H}_s(\mathbf{x}^{[n]} - (\mathrm{diag}(\mathbf{b})\mathbf{\Phi})^T (\mathbf{b} \odot \mathbf{\Phi x}^{[n]})^-), \tag{3.13}$$

where diag($\mathbf{b}$) denotes a square diagonal matrix whose diagonal is vector $\mathbf{b}$. The steps of (3.11) are depicted in Algorithm 3.

Algorithm 3 BIHT-ℓ_2

1. **Inputs:** binary measurements vector $\mathbf{b} \in \{\pm 1\}^M$, measurement matrix $\mathbf{\Phi}$, sparsity level of the signal s, descent step size τ, number of iterations t
2. **Initialization:** Initial estimate $\mathbf{x}^{[0]} = \mathbf{0}$
3. **Iteration:** For $n = 1, \ldots, t$
   (a) **Gradient descent:**
   $\mathbf{z}^{[n]} \leftarrow \mathbf{x}^{[n-1]} - \tau \left(\mathrm{diag}(\mathbf{b})\mathbf{\Phi} \right)^T \left(\mathrm{diag}(\mathbf{b})\mathbf{\Phi x}^{[n-1]} \right)^-$
   (b) **Projection onto "ℓ_0-ball":** $\mathbf{x}^{[n]} \leftarrow \mathcal{H}_s(\mathbf{z}^{[n]})$
4. **Output:** $\hat{\mathbf{x}} = \frac{\mathbf{x}^{[n]}}{\|\mathbf{x}^{[n]}\|_2}$

3.3.3 RFPI

Another approach to signal reconstruction for 1-bit compressive sensing is introduced in [8]. In this method, the recovered signal is obtained by solving minimization program:

$$\begin{aligned}
&\hat{\mathbf{x}} = \arg\min_{\mathbf{x}} \|\mathbf{x}\|_1 \\
&\text{subject to } \mathbf{b} \odot \mathbf{\Phi x} \succeq \mathbf{0} \\
&\text{and} \qquad \|\mathbf{x}\|_2 = 1,
\end{aligned} \tag{3.14}$$

where $\succeq$ denotes element-wise inequality. To solve (3.14) efficiently, a barrier cost function is introduced in [8], which, together with Lagrange multiplier method [21], yields the following approximation of (3.14)

$$\begin{aligned}
&\hat{\mathbf{x}} = \arg\min_{\mathbf{x}} \|\mathbf{x}\|_1 + \lambda \sum_i f\left([\mathbf{b} \odot \mathbf{\Phi x}]_i\right) \\
&\text{subject to} \quad \|\mathbf{x}\|_2 = 1,
\end{aligned} \tag{3.15}$$

where

$$f(x) = \begin{cases} x^2/2, & \text{if } x < 0 \\ 0, & \text{otherwise} \end{cases} \tag{3.16}$$

is the barrier cost function. Note that when λ is sufficiently large, the solution of (3.14) coincides with the solution of (3.15). Since (3.16) is convex and smooth, the gradient descent can be applied to solve the minimization problem (3.15). *Renormalized fixed point iteration* (RFPI) is the algorithm introduced in [8] and solves (3.15). In Algorithm 4 the steps of RFPI are shown. In this algorithm, $\mathbf{x}^{[0]}$ is initialized by $\Phi^{-1}\tilde{\mathbf{b}}/\left\|\Phi^{-1}\tilde{\mathbf{b}}\right\|_2$. The calculation of pseudo-inverse considerably increases the complexity of the algorithm. However, it is shown that random initialization of RFPI converges with high probability [8].

To summarize, we introduced three 1-bit reconstruction algorithms in this chapter. In Table 3.1 an overview of the reconstruction algorithms are shown. As it is obvious in this table, in order to estimate the signal accurately, BIHT and BIHT-ℓ_2 need one more input than RFPI does, which is the sparsity level of the signal, s. We use this characteristic of RFPI as an advantage in the next chapter to design a new reconstruction algorithm that does not require s as an input. In addition, the task of the next chapter is to analyze some other reconstruction algorithms which are robust against the noise in the binary measurements vector.

Algorithm 4 RFPI

1. **Inputs:** vector of 1-bit measurements $\mathbf{b} \in \{\pm 1\}^M$, measuring matrix Φ, number of outer iterations t_1, number of inner iterations t_2

2. **Initialization:** descent step-size δ, $\mathbf{x}^{[0]} = \Phi^{-1}\tilde{\mathbf{b}} / \left\| \Phi^{-1}\tilde{\mathbf{b}} \right\|_2$, initial coefficient $\lambda^{[1]} = M$

3. **Outer iteration:** For $k = 1, \ldots, t_1$

   (a) **Inner iteration:** For $n = 1, \ldots, t_2$

      i. **One-sided quadratic gradient:**
      $\mathbf{s} \leftarrow (\mathrm{diag}(\mathbf{b})\Phi)^T \left(\mathbf{b} \odot \Phi\mathbf{x}^{[n-1]}\right)^-$

      ii. **Gradient projection on sphere surface:**
      $\mathbf{g} \leftarrow \left\langle \mathbf{s}, \mathbf{x}^{[n-1]} \right\rangle \mathbf{x}^{[n-1]} - \mathbf{s}$

      iii. **One-sided quadratic gradient descent:**
      $\mathbf{h} \leftarrow \mathbf{x}^{[n-1]} - \delta\mathbf{g}$

      iv. **Shrinkage (ℓ_1 gradient descent):**
      $[\mathbf{u}]_i \leftarrow \mathrm{sign}\left([\mathbf{h}]_i\right) \max\left\{ |[\mathbf{h}]_i| - \frac{\delta}{\lambda_{[k]}}, 0 \right\}, \text{for all } i$

      v. **Normalization:** $\mathbf{x}^{[n]} \leftarrow \frac{\mathbf{u}}{\|\mathbf{u}\|_2}$

   (b) **Initialize next inner iteration:**
   $\mathbf{x}^{[0]} \leftarrow \mathbf{x}^{[n]}$, $\lambda^{[k+1]} \leftarrow c\lambda^{[k]}$, where c is a fixed constant.

4. **Output:** $\hat{\mathbf{x}} = \mathbf{x}^{[n]}$

Mehod	Formula	Inputs
BIHT	$\arg\min_{\mathbf{x}} \left\| (\mathbf{b} \odot \mathbf{\Phi x})^{-} \right\|_1$ subject to $\|\mathbf{x}\| \leq s$, $\|\mathbf{x}\|_2 = 1$	$\mathbf{\Phi}$, $\mathbf{b}$, s
BIHT-ℓ_2	$\arg\min_{\mathbf{x}} \left\| (\mathbf{b} \odot \mathbf{\Phi x})^{-} \right\|_2$ subject to $\|\mathbf{x}\| \leq s$, $\|\mathbf{x}\|_2 = 1$	$\mathbf{\Phi}$, $\mathbf{b}$, s
RFPI	$\arg\min_{\mathbf{x}} \|\mathbf{x}\|_1$ subject to $\mathbf{b} \odot \mathbf{\Phi x} \succeq \mathbf{0}$, $\|\mathbf{x}\|_2 = 1$	$\mathbf{\Phi}$, $\mathbf{b}$

Table 3.1: Three reconstruction algorithms for 1-bit compressive sensing in the noiseless scenario.

Chapter 4

1-bit compressive sensing in the presence of noise

In the previous chapter, we discussed about 1-bit compressive sensing and the reconstruction algorithms. However, in the case that the binary measurements are contaminated with the noise, the reconstruction algorithms fail to estimate the signal perfectly. We start this chapter by modelling the noise in 1-bit compressive sensing and we introduce two different sources of the noise. Then, we explain some reconstruction algorithms designed to perform robustly against the noise in the binary measurements.

4.1 Noise modelling in 1-bit compressive sensing

4.1.1 Measurement noise

In the case that there is noise in the compressive sensing measurements, we have

$$\tilde{\mathbf{y}} = \mathbf{\Phi}\mathbf{x} + \mathbf{n} \tag{4.1}$$

where $\tilde{\mathbf{y}}$ is the *noisy measurements vector* and $\mathbf{n}$ denotes white Gaussian additive noise vector, i.e., $[\mathbf{n}]_i \sim \mathcal{N}(0, \sigma_n^2)$. After 1-bit quantization of (4.1) we obtain the binary measurements vector contaminated with the measurement noise and the noisy binary measurements vector is denoted by $\tilde{\mathbf{b}}_m$. Hence,

$$\tilde{\mathbf{b}}_m = \text{sign}(\tilde{\mathbf{y}}) = \text{sign}(\mathbf{\Phi}\mathbf{x} + \mathbf{n}) \tag{4.2}$$

In fact the noise in the measurements vector causes sign flips in the binary measurements vector. As the variance of the noise increases it is more likely

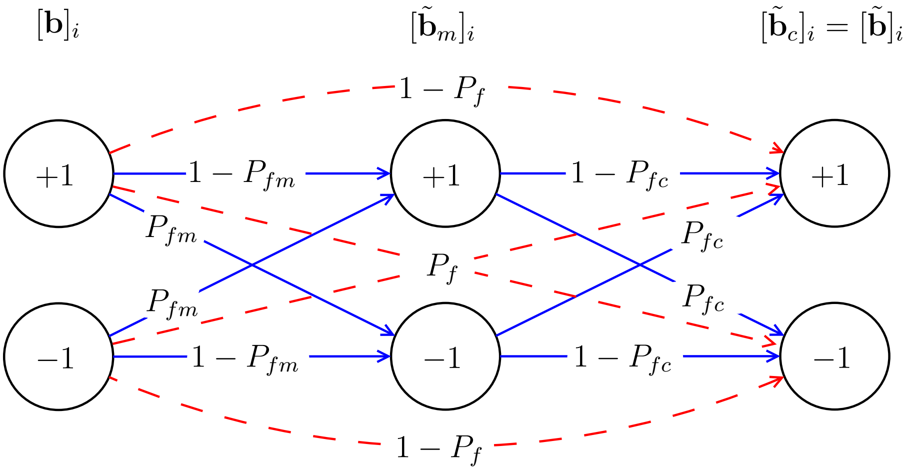

Figure 4.1: Binary symmetric channel model

to occur bit flips in $\tilde{\mathbf{b}}_m$. The probability of bit flip in each bit of $\tilde{\mathbf{b}}_m$ is denoted by P_{fm} and is calculated in Appendix B.

4.1.2 Channel noise

In practice, especially in communications applications, the binary measurements vector $\tilde{\mathbf{b}}_m$ is transmitted through a channel. The noise of this transmission channel causes extra sign flips on the binary measurements. We model the channel by a *binary symmetric channel* (BSC). The probability of sign flips in the BSC is

$$P_{fc} = \mathbb{P}([\tilde{\mathbf{b}}_m]_i = +1 | [\tilde{\mathbf{b}}_c]_i = -1) = \mathbb{P}([\tilde{\mathbf{b}}_m]_i = -1 | [\tilde{\mathbf{b}}_c]_i = +1) \tag{4.3}$$

where $\tilde{\mathbf{b}}_c$ denotes binary measurements vector contaminated with the channel noise.

4.1.3 A combined model for binary noise

As mentioned in the previous section, there are two different sources of the binary noise: the measurement noise and the channel noise. Having the sign flip probability, P_{fm}, caused by measurement noise, we can show the effect of measurement noise by a BSC. Then, we put the physical transmission channel after this model. Therefore, we have two BSC channels connected in serial. As Figure 4.1 depicts, the noiseless binary measurements $\mathbf{b}$ passes through first BSC with sign flip probability P_{fm} then its output is put to the second BSC which is the physical channel with sign flip probability P_{fc}.

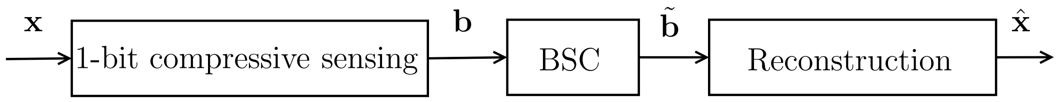

Figure 4.2: 1-bit compressive sensing in the presence of the noise

$\tilde{\mathbf{b}}$ denotes the final noisy binary data after the measurement noise and the channel noise.

We replace these two BSCs by a simple equivalent BSC with sign flip probability P_f. The value of P_f given P_{fm} and P_{fc} can be obtained from

$$\begin{pmatrix} 1-P_f & P_f \\ P_f & 1-P_f \end{pmatrix} = \begin{pmatrix} 1-P_{fm} & P_{fm} \\ P_{fm} & 1-P_{fm} \end{pmatrix} \begin{pmatrix} 1-P_{fc} & P_{fc} \\ P_{fc} & 1-P_{fc} \end{pmatrix} \tag{4.4}$$

and

$$P_f = P_{fc}(1-P_{fm}) + P_{fm}(1-P_{fc}). \tag{4.5}$$

The approximate number of the total sign flips between $\mathbf{b}$ and $\tilde{\mathbf{b}}$ which is denoted by L can be obtain from

$$L \approx MP_f. \tag{4.6}$$

In fact, L is a measure of the noise level in 1-bit compressive sensing. Note that as M tends to infinity, L converges to MP_f.

4.2 Iterative reconstruction algorithms for 1-bit compressive sensing in the presence of noise

The block diagram of 1-bit compressive sensing in the presence of noise is shown in Figure 4.2. The task of reconstruction algorithms in the presence of noise is to reconstruct the signal form the noisy binary measurements $\tilde{\mathbf{b}}$. In the first part of this section, we explain an algorithm which reconstructs the signal in the presence of noise. Then, we introduce our reconstruction algorithm that works robustly against the binary noise and does not require sparsity level of the signal as an input.

4.2.1 Adaptive outlier pursuit

AOP and AOP-ℓ_2

In [10], a reconstruction algorithm called *adaptive outlier pursuit* (AOP) has been proposed. In this algorithm, a binary vector $\mathbf{\Lambda}$ is defined in which the position of 0's shows the position of the sign flips and the position of 1's shows the position of the unchanged bits in $\tilde{\mathbf{b}}$, i.e., $[\boldsymbol{\Lambda}]_i \in \{0,1\}^M$. Therefore, the number of sign flips in $\tilde{\mathbf{b}}$ can be obtained from

$$L = \sum_i (1 - [\boldsymbol{\Lambda}]_i). \tag{4.7}$$

Given the number of sign flips, L, and the sparsity level of the signal, s, AOP tries to solve the following optimization problem

$$\begin{aligned}
(\hat{\mathbf{x}}, \hat{\boldsymbol{\Lambda}}) = \arg\min_{\mathbf{x},\boldsymbol{\Lambda}} & \left\| \left(\boldsymbol{\Lambda} \odot \tilde{\mathbf{b}} \odot \boldsymbol{\Phi}\mathbf{x} \right)^{-} \right\|_1 \\
\text{subject to} \quad & \sum_i (1 - [\boldsymbol{\Lambda}]_i) \leq L \\
& \|\mathbf{x}\|_0 \leq s \\
& \|\mathbf{x}\|_2 = 1
\end{aligned} \tag{4.8}$$

where $\hat{\mathbf{x}}$ denotes the estimated signal and $\hat{\boldsymbol{\Lambda}}$ denotes the estimated binary vector. Note that in the noiseless case $[\boldsymbol{\Lambda}]_i = 1$ for all i and the problem in (4.8) converts to BIHT. AOP solves (4.8) by iterating between two following steps:
Step 1: given $\hat{\boldsymbol{\Lambda}}$ find

$$\begin{aligned}
\hat{\mathbf{x}} = \arg\min_{\mathbf{x}} & \left\| \left(\hat{\boldsymbol{\Lambda}} \odot \tilde{\mathbf{b}} \odot \boldsymbol{\Phi}\mathbf{x} \right)^{-} \right\|_1 \\
\text{subject to} \quad & \|\mathbf{x}\|_0 \leq s \\
& \|\mathbf{x}\|_2 = 1
\end{aligned} \tag{4.9}$$

Step 2: given $\hat{\mathbf{x}}$ find

$$\begin{aligned}
\hat{\boldsymbol{\Lambda}} = \arg\min_{\boldsymbol{\Lambda}} & \left\| \left(\boldsymbol{\Lambda} \odot \tilde{\mathbf{b}} \odot \boldsymbol{\Phi}\hat{\mathbf{x}} \right)^{-} \right\|_1 \\
\text{subject to} \quad & \sum_i (1 - [\boldsymbol{\Lambda}]_i) \leq L
\end{aligned} \tag{4.10}$$

First $\hat{\mathbf{x}}$ is determined by solving (4.9), based on the current estimation of $\hat{\boldsymbol{\Lambda}}$. In other words, AOP tries to minimize

$$\sum_{i \in V} [(\tilde{\mathbf{b}} \odot \boldsymbol{\Phi}\mathbf{x})^{-}]_i, \tag{4.11}$$

where $\mathbf{x}$ is s-sparse, $V = \mathrm{Supp}(\hat{\boldsymbol{\Lambda}})$ and $\mathrm{Supp}(\cdot)$ gives the indices of the non-zero elements in the argument. In the second step, $\hat{\boldsymbol{\Lambda}}$ is updated by solving

Algorithm 5 AOP

1. **Inputs:** Measurement signs $\tilde{\mathbf{b}} \in \{\pm 1\}^M$, Measurement matrix $\mathbf{\Phi}$, Signal sparsity s, Constant τ
2. **Initialization:** Initial estimate $\mathbf{x}^{[0]} = \mathbf{\Phi}^T \tilde{\mathbf{b}} / \left\| \mathbf{\Phi}^T \tilde{\mathbf{b}} \right\|_2$
3. **Iteration:** For $n = 1, \dots, t$
   (a) **Update support:** $V \leftarrow \mathrm{Supp}(\mathbf{\Lambda})$
   (b) **Gradient descent:**
   $\mathbf{z}^{[n]} \leftarrow \mathbf{x}^{[n-1]} - \tau \left(\mathbf{\Phi}_{[V,:]}\right)^T \left(\mathrm{sign}\left(\mathbf{\Phi}_{[V,:]}\mathbf{x}^{[n-1]}\right) - \tilde{\mathbf{b}}_V\right)$
   (c) **Projection onto "ℓ_0-ball":** $\mathbf{x}^{[n]} \leftarrow \mathcal{H}_s(\mathbf{z}^{[n]})$
   (d) **Update $\mathbf{\Lambda}$:** Update $\mathbf{\Lambda}$ from (4.12)
4. **Output:** $\hat{\mathbf{x}} = \frac{\mathbf{x}^{[n]}}{\left\|\mathbf{x}^{[n]}\right\|_2}$

(4.10), based on the new estimation of $\hat{\mathbf{x}}$. In [10], it is shown that (4.10) can be solved analytically and its solution is given by

$$\left[\hat{\mathbf{\Lambda}}\right]_i = \begin{cases} 0, & \text{if } \left[\left(\tilde{\mathbf{b}} \odot \Phi\hat{\mathbf{x}}\right)^-\right]_i \geq \beta \\ 1, & \text{otherwise.} \end{cases} \tag{4.12}$$

Here, β is the Lth largest entry of the vector $\left(\tilde{\mathbf{b}} \odot \mathbf{\Phi}\hat{\mathbf{x}}\right)^-$. In Algorithm 5, the steps of AOP is illustrated. This algorithm is initialized with $\mathbf{x}^{[0]} = \mathbf{\Phi}^T\tilde{\mathbf{b}} / \left\|\mathbf{\Phi}^T\tilde{\mathbf{b}}\right\|_2$ and $\mathbf{\Phi}_{[V,:]}$ denotes a sub-matrix of $\mathbf{\Phi}$ which is restricted to the rows of $\mathbf{\Phi}$ in set V.

Another version of AOP is AOP-ℓ_2 which minimizes $\left\|\left(\mathbf{\Lambda} \odot \tilde{\mathbf{b}} \odot \mathbf{\Phi}\mathbf{x}\right)^-\right\|_2$ instead of $\left\|\left(\mathbf{\Lambda} \odot \tilde{\mathbf{b}} \odot \mathbf{\Phi}\mathbf{x}\right)^-\right\|_1$. Therefore, AOP-$\ell_2$ is basically derived from BIHT-ℓ_2 and the steps are the same as in Algorithm 5 while the step (b) is replaced by

$$\mathbf{z}^{[n]} = \mathbf{x}^{[n-1]} - \left(\mathrm{diag}(\tilde{\mathbf{b}})_{[V,:]}\mathbf{\Phi}_{[V,:]}\right)^T \left(\mathrm{diag}(\tilde{\mathbf{b}})_{[V,:]}\mathbf{\Phi}_{[V,:]}\mathbf{x}^{[n-1]}\right)^- . \tag{4.13}$$

AOP and AOP-ℓ_2 with sign flips

Another version of AOP is called *adaptive outlier pursuit with sign flips* (AOP-f) [10] which applies binary vector $\mathbf{\Omega} \in \{\pm 1\}^M$ where $\tilde{\mathbf{b}} \odot \mathbf{b} = \mathbf{\Omega}$. That is, the position of -1's shows the position of flipped bits and the position of 1's specifies the position of unchanged bits in $\tilde{\mathbf{b}}$. Therefore,

$$[\mathbf{\Omega}]_i = 2\,[\mathbf{\Lambda}]_i - 1 \tag{4.14}$$

In fact, if $\mathbf{\Omega}$ is estimated perfectly, we have

$$\mathbf{b} = \mathbf{\Omega} \odot \tilde{\mathbf{b}}. \tag{4.15}$$

and

$$L = \frac{1}{2}\sum_i (1 - [\mathbf{\Omega}]_i). \tag{4.16}$$

AOP-f is obtained by replacing $\mathbf{b}$ with $\mathbf{\Omega} \odot \tilde{\mathbf{b}}$ (which is the flipped version of $\tilde{\mathbf{b}}$) in BIHT. Both $\mathbf{x}$ and $\mathbf{\Omega}$ are estimated in each iteration. The minimization problem that AOP-f solves is as follows:

$$\begin{aligned}
(\hat{\mathbf{x}}, \hat{\mathbf{\Omega}}) = \arg\min_{\mathbf{x},\mathbf{\Omega}} & \left\| \left(\mathbf{\Omega} \odot \tilde{\mathbf{b}} \odot \mathbf{\Phi}\mathbf{x} \right)^{-} \right\|_1 \\
\text{subject to} \quad & \frac{1}{2}\sum_i (1 - [\mathbf{\Omega}]_i) \le L \\
& \|\mathbf{x}\|_0 \le s \\
& \|\mathbf{x}\|_2 = 1
\end{aligned} \tag{4.17}$$

The steps of solving (4.17) are the same as the steps in (4.8). That is, first by fixing $\hat{\mathbf{\Omega}}$, AOP-f estimates $\hat{\mathbf{x}}$. Hence,

$$\begin{aligned}
\hat{\mathbf{x}} = \arg\min_{\mathbf{x}} & \left\| \left(\hat{\mathbf{\Omega}} \odot \tilde{\mathbf{b}} \odot \mathbf{\Phi}\mathbf{x} \right)^{-} \right\|_1 \\
\text{subject to} \quad & \|\mathbf{x}\|_0 \le s \\
& \|\mathbf{x}\|_2 = 1
\end{aligned} \tag{4.18}$$

Then, AOP-f updates $\hat{\mathbf{\Omega}}$ given $\hat{\mathbf{x}}$ obtained from previous step. Therefore,

$$\begin{aligned}
\hat{\mathbf{\Omega}} = \arg\min_{\mathbf{\Omega}} & \left\| \left(\mathbf{\Omega} \odot \tilde{\mathbf{b}} \odot \mathbf{\Phi}\hat{\mathbf{x}} \right)^{-} \right\|_1 \\
\text{subject to} \quad & \frac{1}{2}\sum_i (1 - [\mathbf{\Omega}]_i) \le L.
\end{aligned} \tag{4.19}$$

Algorithm 6 AOP-f

1. **Inputs:** Measurement signs $\tilde{\mathbf{b}} \in \{\pm 1\}^M$, Measurement matrix $\mathbf{\Phi}$, Signal sparsity s, Constant τ

2. **Initialization:** Initial estimate $\mathbf{x}^{[0]} = \mathbf{\Phi}^T\tilde{\mathbf{b}}/\left\|\mathbf{\Phi}^T\tilde{\mathbf{b}}\right\|_2$

3. **Iteration:** For $n = 1, \ldots, t$

   (a) **Gradient Descent:** $\mathbf{z}^{[n]} \leftarrow \mathbf{x}^{[n-1]} - \tau\mathbf{\Phi}^T\left(\text{sign}\left(\mathbf{\Phi}\mathbf{x}^{[n-1]}\right) - \tilde{\mathbf{b}}\right)$

   (b) **Projection onto "ℓ_0-ball":** $\mathbf{x}^{[n]} \leftarrow \mathcal{H}_s(\mathbf{z}^{[n]})$

   (c) **Update $\mathbf{\Omega}$:** Update $\mathbf{\Omega}$ from (4.20)

   (d) **Update $\tilde{\mathbf{b}}$:** $\tilde{\mathbf{b}} \leftarrow \mathbf{\Omega} \odot \tilde{\mathbf{b}}$

4. **Output:** $\hat{\mathbf{x}} = \frac{\mathbf{x}^{[n]}}{\left\|\mathbf{x}^{[n]}\right\|_2}$

The estimation of $\hat{\mathbf{\Omega}}$ in the second step is given by

$$\left[\hat{\mathbf{\Omega}}\right]_i = \begin{cases} -1, & \text{if } \left[\left(\tilde{\mathbf{b}} \odot \Phi\hat{\mathbf{x}}\right)^-\right]_i \geq \beta \\ 1, & \text{otherwise} \end{cases} \tag{4.20}$$

where β has the same value as in (4.12). Like in AOP, we can replace ℓ_2-norm by ℓ_1-norm which yields AOP-ℓ_2-f. Note that since elements in $\left(\mathbf{\Omega} \odot \tilde{\mathbf{b}} \odot \mathbf{\Phi}\hat{\mathbf{x}}\right)^-$ are non-negative values, the estimation of $\hat{\mathbf{\Omega}}$ in AOP-f-ℓ_2 is also given by (4.20). If the binary measurements vector is noiseless then $[\mathbf{\Omega}]_i = 1$ for all i and AOP-f (AOP-ℓ_2-f) converts to BIHT (BIHT-ℓ_2). Algorithm 6 shows the steps in AOP-f. To convert AOP-f to AOP-ℓ_2-f, we just need to replace step (a) by

$$\mathbf{z}^{[n]} = \mathbf{x}^{[n-1]} - \left(\text{diag}(\tilde{\mathbf{b}})\mathbf{\Phi}\right)^T\left(\text{diag}(\tilde{\mathbf{b}})\mathbf{\Phi}\mathbf{x}^{[n-1]}\right)^-. \tag{4.21}$$

4.2.2 Noise-adaptive renormalized fixed point iterative

In this section, we introduce *noise-adaptive renormalized fixed point iterative* (NARFPI) which is a reconstruction algorithm mostly derived from RFPI.

By applying (4.15) we modify (3.14) to account for bit flips as follows:

$$
\begin{aligned}
(\hat{\mathbf{x}}, \hat{\mathbf{\Omega}}) = \arg\min_{\mathbf{x},\mathbf{\Omega}} \|\mathbf{x}\|_1& \\
\text{subject to} \quad & \mathbf{\Omega} \odot \tilde{\mathbf{b}} \odot \Phi\mathbf{x} \succeq \mathbf{0} \\
& \frac{1}{2}\sum_i (1 - [\mathbf{\Omega}]_i) \leq L \\
& \|\mathbf{x}\|_2 = 1.
\end{aligned} \tag{4.22}
$$

To solve (4.22) efficiently, we can apply the same relaxation step as in (3.15) and approximate (4.22) by

$$
\begin{aligned}
(\hat{\mathbf{x}}, \hat{\mathbf{\Omega}}) = \arg\min_{\mathbf{x},\mathbf{\Omega}} & \|\mathbf{x}\|_1 + \lambda \sum_i f([\mathbf{\Omega} \odot \tilde{\mathbf{b}} \odot \mathbf{\Phi}\mathbf{x}]_i) \\
\text{subject to} \quad & \frac{1}{2}\sum_i (1 - [\mathbf{\Omega}]_i) \leq L \\
& \|\mathbf{x}\|_2 = 1.
\end{aligned} \tag{4.23}
$$

The optimization problem in (4.23) is still non-convex and consists of a combination of discrete and continuous variables. Similarly to the approach in [8] to solve (3.15), we use two steps algorithm to find $\hat{\mathbf{\Omega}}$ and $\hat{\mathbf{x}}$ in (4.23). In the first step, $\hat{\mathbf{\Omega}}$ is fixed and the algorithm finds the optimum $\hat{\mathbf{x}}$ as follows:

$$
\begin{aligned}
\hat{\mathbf{x}} = \arg\min_{\mathbf{x}} & \|\mathbf{x}\|_1 + \lambda \sum_i f([\hat{\mathbf{\Omega}} \odot \tilde{\mathbf{b}} \odot \mathbf{\Phi}\mathbf{x}]_i) \\
\text{subject to} \quad & \|\mathbf{x}\|_2 = 1.
\end{aligned} \tag{4.24}
$$

Note that the only difference between (3.15) and (4.24) is that $\mathbf{b}$ is replaced by $\tilde{\mathbf{b}} \odot \hat{\mathbf{\Omega}}$. Hence, we can use RFPI to solve (4.24). In the second step, we use $\hat{\mathbf{x}}$ obtained from (4.24), to find $\hat{\mathbf{\Omega}}$ as follows:

$$
\begin{aligned}
\hat{\mathbf{\Omega}} = \arg\min_{\mathbf{\Omega}} & \sum_i f([\mathbf{\Omega} \odot \tilde{\mathbf{b}} \odot \mathbf{\Phi}\hat{\mathbf{x}}]_i) \\
\text{subject to} \quad & \frac{1}{2}\sum_i (1 - [\mathbf{\Omega}]_i) \leq L.
\end{aligned} \tag{4.25}
$$

We can rewrite (4.25) as

$$
\begin{aligned}
\hat{\mathbf{\Omega}} = \arg\min_{\mathbf{\Omega}} & \left\| \left(\mathbf{\Omega} \odot \tilde{\mathbf{b}} \odot \mathbf{\Phi}\hat{\mathbf{x}} \right)^{-} \right\|_2 \\
\text{subject to} \quad & \frac{1}{2}\sum_i (1 - [\mathbf{\Omega}]_i) \leq L.
\end{aligned} \tag{4.26}
$$

The minimization in (4.26) is identical to the second step of AOP-ℓ_2-f (when ℓ_1-norm is replaced by ℓ_2-norm in (4.19)). Therefore, the solution of (4.26) is (4.20). The details of NARFPI is shown in Algorithm 7. In Table 4.1, the algorithms designed for 1-bit compressive sensing in the presence of the binary noise are described briefly. The main advantage of NARFPI in comparison to the other algorithms is that it does not require a priori knowledge of s as an input.

Algorithm 7 NARFPI

1. **Inputs:** vector of 1-bit measurements $\tilde{\mathbf{b}} \in \{\pm 1\}^M$, measuring matrix Φ, number of bit flips L, number of outer iterations t_1, number of inner iterations t_2
2. **Initialization:** descent step-size δ, initial estimate $[\mathbf{\Omega}]_i = 1$ for all i, $\mathbf{x}^{[0]} = \Phi^{-1}\tilde{\mathbf{b}} / \left\|\Phi^{-1}\tilde{\mathbf{b}}\right\|_2$, initial coefficient $\lambda^{[1]} = M$
3. **Outer iteration:** For $k = 1, \ldots, t_1$
   (a) **Inner iteration:** For $n = 1, \ldots, t_2$
      i. **One-sided quadratic gradient:**
      $\mathbf{s} \leftarrow \left(\mathrm{diag}(\tilde{\mathbf{b}})\Phi\right)^T \left(\tilde{\mathbf{b}} \odot \Phi\mathbf{x}^{[n-1]}\right)^-$
      ii. **Gradient projection on sphere surface:**
      $\mathbf{g} \leftarrow \left\langle \mathbf{s}, \mathbf{x}^{[n-1]} \right\rangle \mathbf{x}^{[n-1]} - \mathbf{s}$
      iii. **One-sided quadratic gradient descent:**
      $\mathbf{h} \leftarrow \mathbf{x}^{[n-1]} - \delta \mathbf{g}$
      iv. **Shrinkage (ℓ_1 gradient descent):**
      $[\mathbf{u}]_i \leftarrow \mathrm{sign}\left([\mathbf{h}]_i\right) \max\left\{|[\mathbf{h}]_i| - \frac{\delta}{\lambda_{[k]}}, 0\right\}$, for all i
      v. **Normalization:** $\mathbf{x}^{[n]} \leftarrow \frac{\mathbf{u}}{\|\mathbf{u}\|_2}$
   (b) **Find the location of noisy bits and flip them:**
   Update $\mathbf{\Omega}$ from (4.20). $\tilde{\mathbf{b}} \leftarrow \mathbf{\Omega} \odot \tilde{\mathbf{b}}$.
   (c) **Initialize next inner iteration:**
   $\mathbf{x}^{[0]} \leftarrow \mathbf{x}^{[n]}$, $\lambda^{[k+1]} \leftarrow c\lambda^{[k]}$, where c is a fixed constant.
4. **Output:** $\hat{\mathbf{x}} = \mathbf{x}^{[n]}$

Mehod	Formula	Inputs
AOP	$\underset{\mathbf{x},\boldsymbol{\Lambda}}{\arg\min} \left\| \left(\boldsymbol{\Lambda} \odot \tilde{\mathbf{b}} \odot \boldsymbol{\Phi}\mathbf{x}\right)^{-} \right\|_1$ subject to $\sum_i (1 - [\boldsymbol{\Lambda}]_i) \leq L$, $\|\mathbf{x}\|_0 \leq s$, $\|\mathbf{x}\|_2 = 1$	$\boldsymbol{\Phi}$, $\tilde{\mathbf{b}}$, s, L
AOP-ℓ_2	$\underset{\mathbf{x},\boldsymbol{\Lambda}}{\arg\min} \left\| \left(\boldsymbol{\Lambda} \odot \tilde{\mathbf{b}} \odot \boldsymbol{\Phi}\mathbf{x}\right)^{-} \right\|_2$ subject to $\sum_i (1 - [\boldsymbol{\Lambda}]_i) \leq L$, $\|\mathbf{x}\|_0 \leq s$, $\|\mathbf{x}\|_2 = 1$	$\boldsymbol{\Phi}$, $\tilde{\mathbf{b}}$, s, L
AOP-f	$\underset{\mathbf{x},\boldsymbol{\Omega}}{\arg\min} \left\| \left(\boldsymbol{\Omega} \odot \tilde{\mathbf{b}} \odot \boldsymbol{\Phi}\mathbf{x}\right)^{-} \right\|_1$ subject to $\frac{1}{2}\sum_i (1 - [\boldsymbol{\Omega}]_i) \leq L$, $\|\mathbf{x}\|_0 \leq s$, $\|\mathbf{x}\|_2 = 1$	$\boldsymbol{\Phi}$, $\tilde{\mathbf{b}}$, s, L
AOP-f-ℓ_2	$\underset{\mathbf{x},\boldsymbol{\Omega}}{\arg\min} \left\| \left(\boldsymbol{\Omega} \odot \tilde{\mathbf{b}} \odot \boldsymbol{\Phi}\mathbf{x}\right)^{-} \right\|_2$ subject to $\frac{1}{2}\sum_i (1 - [\boldsymbol{\Omega}]_i) \leq L$, $\|\mathbf{x}\|_0 \leq s$, $\|\mathbf{x}\|_2 = 1$	$\boldsymbol{\Phi}$, $\tilde{\mathbf{b}}$, s, L
NARFPI	$\underset{\mathbf{x},\boldsymbol{\Omega}}{\arg\min} \|\mathbf{x}\|_1$ subject to $\boldsymbol{\Omega} \odot \tilde{\mathbf{b}} \odot \boldsymbol{\Phi}\mathbf{x} \succeq \mathbf{0}$, $\frac{1}{2}\sum_i (1 - [\boldsymbol{\Omega}]_i) \leq L$, $\|\mathbf{x}\|_2 = 1$	$\boldsymbol{\Phi}$, $\tilde{\mathbf{b}}$, L

Table 4.1: Five reconstruction algorithms for 1-bit compressive sensing in the presence of the binary noise.

Chapter 5

Simulations and numerical results

In this chapter, we simulate the 1-bit compressive sensing reconstruction algorithms and analyze their performances in the noiseless and the noisy scenarios. The quality of reconstruction is measured in terms of the *received signal to noise ratio* (RSNR) defined as:

$$\text{RSNR} = \frac{\mathbb{E}\left(\|\mathbf{x}\|_2^2\right)}{\mathbb{E}\left(\|\hat{\mathbf{x}} - \mathbf{x}\|_2^2\right)}. \tag{5.1}$$

Throughout this chapter the deimension of $\mathbf{x}$ is $N = 1000$. The position of non-zero elements in $\mathbf{x}$ is chosen uniformly at random and the amplitude of non-zero elements is generated according to zero-mean Gaussian variable with unite variance. The $M \times N$ measuring matrix Φ has independent entries following a zero-mean Gaussian distribution with variance $1/M$, i.e., $\phi_{i,j} \sim \mathcal{N}(0, 1/M)$. We choose the number of binary measurements from multiples of 100 between 100 to 2000. This setting is beyond the classical compressive sensing goal of few measurements, i.e., $M \ll N$. Note that, we can afford more measurements for a same bit budget compared to more sophisticated quantized compressive sensing approaches. In other words, in 1-bit compressive sensing each measurement is shown by one bit while in other quantized compressive sensing each measurement is shown by two or more bit. Therefore, 1-bit compressive sensing gives the most number of measurements in comparison to others given a fixed number of bits. In the case that the algorithms need the value of L as an input, we feed them by MP_f which is the estimated value of L (see (4.6)). Moreover, we set the number of iterations $t = 1000$, $t_1 = 20$ and $t_2 = 200$.

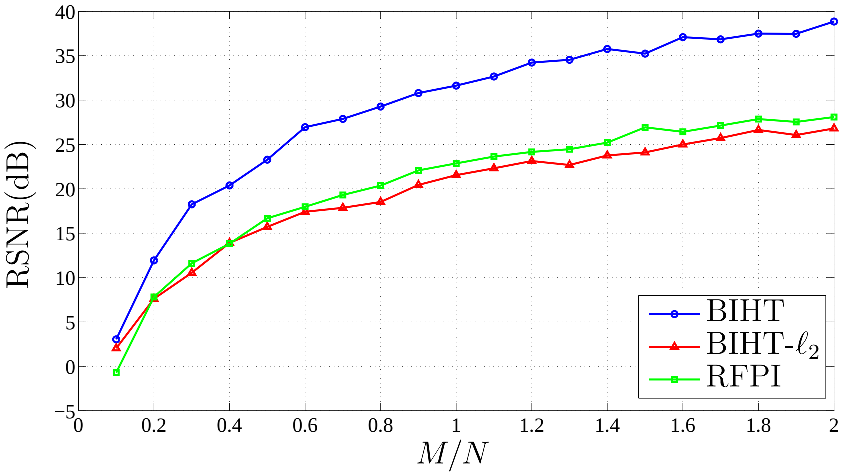

Figure 5.1: The performance of BIHT, BIHT-ℓ_2 and RFPI when $P_f = 0$

5.1 Algorithms designed for noiseless 1-bit compressive sensing

In this section, we simulate BIHT, BIHT-ℓ_2 and RFPI in three different binary noise levels. The sparsity level of $\mathbf{x}$ is set to $s = 10$. We set the probability of bit flips to 0, 1% and 3%. The performance of the three algorithms is averaged over 100 realizations for each M/N. In Figures 5.1, 5.2 and 5.3, the RSNR(dB) of the three algorithms is shown respectively for $P_f = 0$, $P_f = 1\%$ and $P_f = 3\%$. Generally, as P_f increases, the overall reconstruction performance of these three algorithms decreases significantly. When $P_f = 0$, the performance of BIHT is considerably higher than BIHT-ℓ_2 and RFPI. However, as the probability of sign flips increases BIHT-ℓ_2 outperforms BIHT and RFPI. This superior performance of BIHT-ℓ_2 in the presence of the noise claims that for scenarios with high level of binary noise, BIHT-ℓ_2 has the best reconstruction quality among the 1-bit reconstruction algorithms designed for the noiseless case.

5.2 Algorithms designed for noisy 1-bit compressive sensing

In [10], it is shown that the performance of AOP (AOP-ℓ_2) is almost identical to the performance of AOP-f (AOP-f-ℓ_2). Therefore, for the sake of simplicity, we just evaluate the performance of AOP-f (AOP-f-ℓ_2) through out this

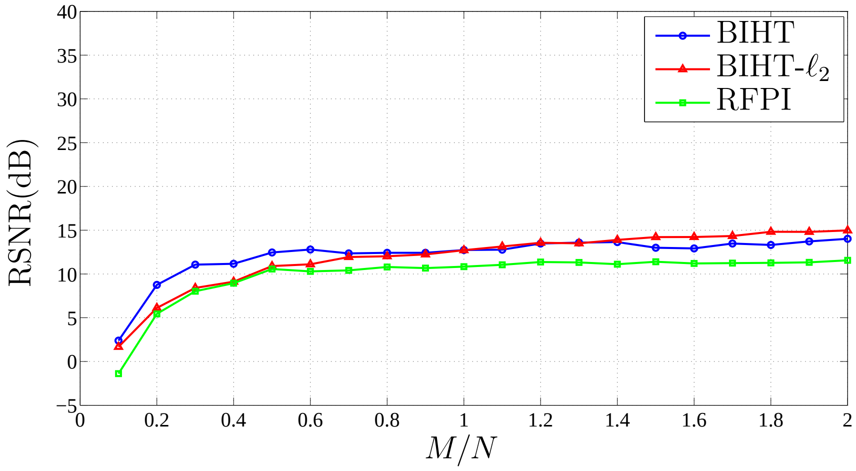

Figure 5.2: The performance of BIHT, BIHT-ℓ_2 and RFPI when $P_f = 1\%$

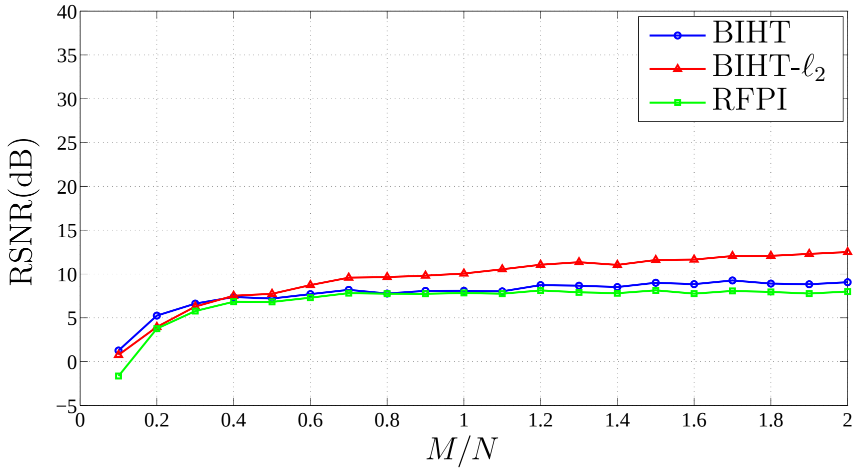

Figure 5.3: The performance of BIHT, BIHT-ℓ_2 and RFPI when $P_f = 3\%$

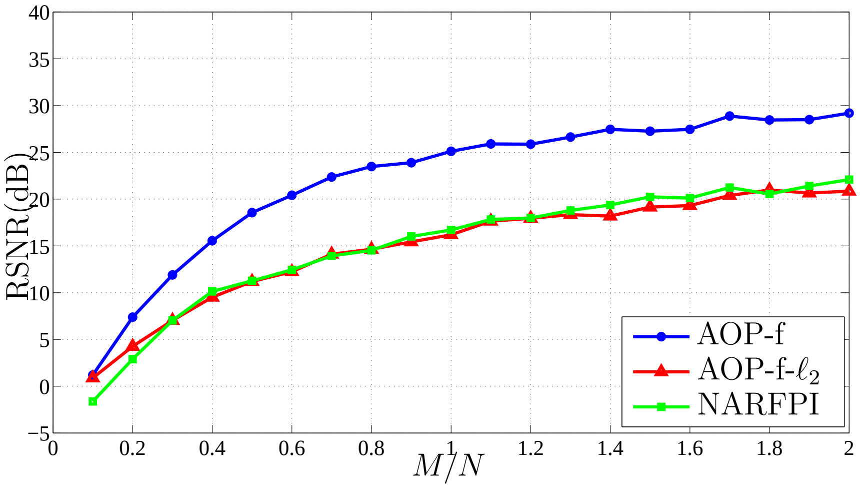

Figure 5.4: The performance of AOP-f, AOP-f-ℓ_2 and NARFPI when $P_f = 3\%$

chapter.

5.2.1 Signals with fixed sparsity level

Similarly to the previous section, the sparsity level of $\mathbf{x}$ is set to $s = 10$. We simulate AOP-f, AOP-f-ℓ_2 and NARFPI in the scenario that $P_f = 3\%$. In Figure 5.4, the performance of the three algorithms are shown by RSNR(dB). AOP-f outperforms NARFPI and AOP-f-ℓ_2. In addition, the performance of AOP-f-ℓ_2 is almost identical to the performance of NARFPI since both of these algorithms try to minimize an ℓ_2-norm.

5.2.2 Signals with random sparsity level

In practice, the exact sparsity level of the signal is not known. As we mentioned before AOP-f and AOP-f-ℓ_2 need a priori knowledge of sparsity level of the signal to be reconstructed as an input. In this section, we simulate the case in which sparsity level of the signal varies randomly based on discrete truncated triangular distribution with mean 10 and $s \in [1, 19]$. The *probability mass function* (PMF) of the random s for three different σ_s^2 is shown in Figure 5.5.

We simulate RFPI, AOP-f, AOP-f-ℓ_2 and NARFPI when $M/N = 2$ and s is random based on the triangular distribution. The probability of sign flips is set to $P_f = 3\%$. Since the mean of s is 10, we put 10 as an estimated s

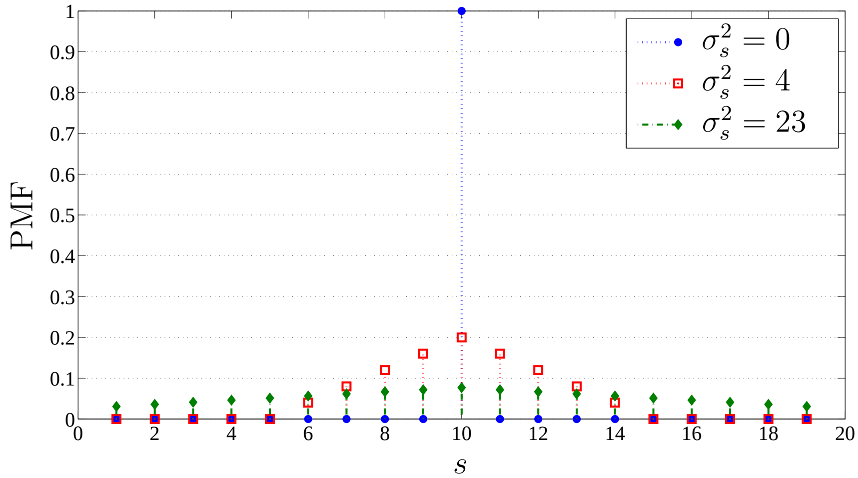

Figure 5.5: The PMF of truncated triangular distribution of s for three different variances

into AOP-f and AOP-f-ℓ_2. In Figure 5.6 the average performance of the four algorithms over 100 realizations for each σ_s^2 is shown. As it is illustrated, the performance of NARFPI is constant and independent of σ_s^2. RFPI exhibits also a constant RSNR as σ_s^2 varies, but its performance is poor because of the presence of bit flips. In contrast, the reconstruction quality of AOP-f and AOP-f-ℓ_2 decreases as deviation of s from its mean increases. When $\sigma_s^2 > 10$, NARFPI outperforms all the other algorithms.

To investigate whether NARFPI apparent superior performance occurs also for other M values, we consider another scenario in which s is fixed to a value between 1 to 19 (but AOP-f and AOP-f-ℓ_2 is still given 10 as estimate) and consider different values of M. The other parameters in this numerical experiment are the same as in the previous simulations. We plot 1/(RSNR) (i.e., the reconstruction error) in linear scale as a function of s for NARFPI (Figure 5.7), AOP-f (Figure 5.8) and AOP-f-ℓ_2 (Figure 5.9).

As expected, the reconstruction error of AOP-f and AOP-f-ℓ_2 is almost constant for $s \leq 10$ but appears to grow faster than linearly in s when s exceeds 10. The error growth rate for $10 \leq s$ in AOP-f is considerably faster than the error growth rate in AOP-f-ℓ_2. This behaviour seems natural given that AOP-f (AOP-f-ℓ_2) minimizes the ℓ_1-norm (ℓ_2-norm) of $\mathbf{x}$ under the constraint that $\|\mathbf{x}\|_0 \leq s$ and that we give $s = 10$ to AOP-f (AOP-f-ℓ_2) as estimate of the signal sparsity level. By comparing Figures 5.7, 5.8 and 5.9, we see that in the regime where the number of measurements is large compared to the signal dimension (e.g., $M/N = 2$), NARFPI outperforms

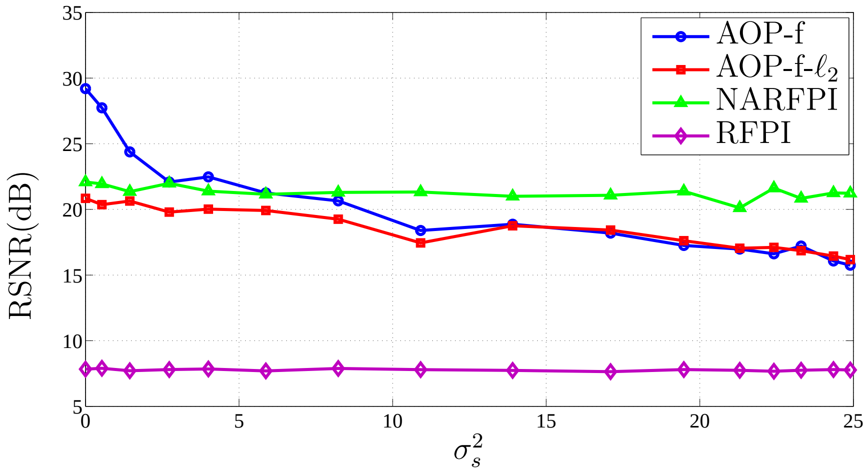

Figure 5.6: The performance of RFPI, AOP-f, AOP-f-ℓ_2 and NARFPI when $P = 3\%$ and s is random based on triangular distribution

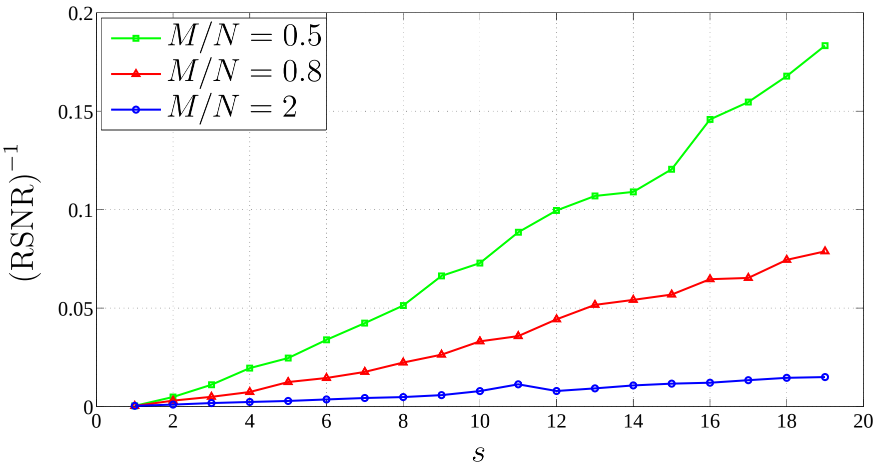

Figure 5.7: The estimation error of NARFPI as a function of the number of binary measurements M and of the sparsity level s of $\mathbf{x}$

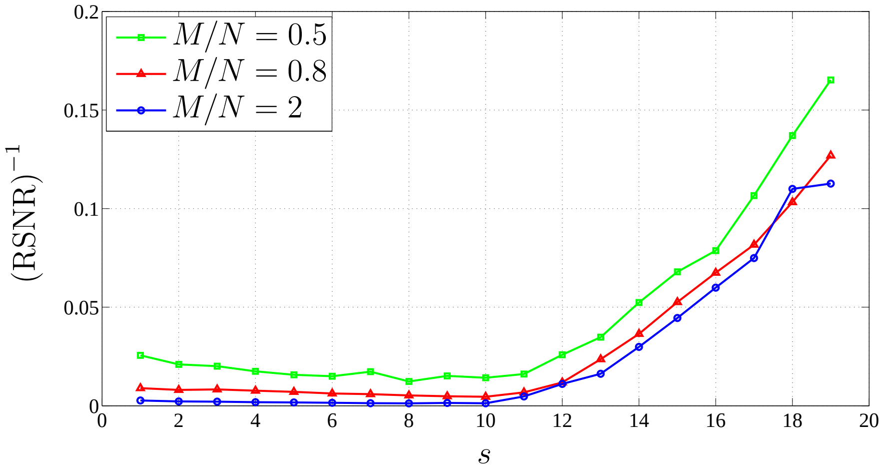

Figure 5.8: The estimation error of AOP-f as a function of the number of binary measurements M and of the sparsity level s of $\mathbf{x}$

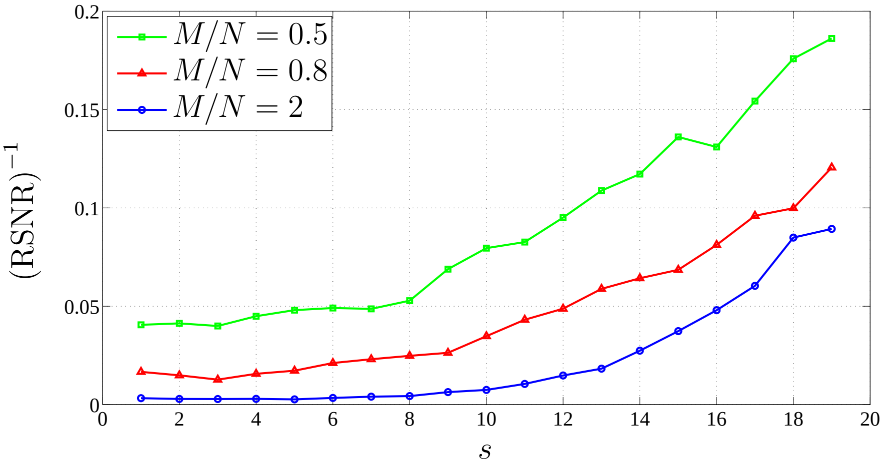

Figure 5.9: The estimation error of AOP-f-ℓ_2 as a function of the number of binary measurements M and of the sparsity level s of $\mathbf{x}$

AOP-f and AOP-f-ℓ_2. However, in the regime where the number of measurements is small compared to the signal dimension (e.g., $M/N = 0.5$), AOP-f outperforms NARFPI for $s > 10$.

Chapter 6

Conclusion

In this thesis, we discussed the general compressive sensing problem and the conditions on measuring matrix $\mathbf{\Phi}$ which ensures the uniqueness of the reconstructed signal through compressive sensing reconstruction algorithms. We showed that RIP holds for a random matrix $\mathbf{\Phi}$ when: 1)the entries of $\mathbf{\Phi}$ are strictly sub-Gaussian and 2) the number of rows in $\mathbf{\Phi}$ is greater than a particular value (related to the sparsity level and the dimension of the signal). Therefore, $\mathbf{\Phi}$ can be applied in compressive sensing and signals measured through this class of matrices can be reconstructed perfectly.

Furthermore, we focused on a quantized version of compressive sensing problems, which is 1-bit compressive sensing. We investigated several 1-bit compressive sensing reconstruction algorithms (BIHT, BIHT-ℓ_2 and RFPI) for noiseless scenario. We modelled the measurement and the channel noise in 1-bit compressive sensing and discussed four reconstruction algorithms (AOP, AOP-ℓ_2, AOP-f, AOP-f-ℓ_2) which are designed to work robustly in the presence of the noise. After that, we introduced our contribution, which is NARFPI, an algorithm obtained by merging RFPI and AOP-f. The main advantage of NARFPI over the previously introduced 1-bit compressive algorithms is that NARFPI does not require a priori knowledge of the sparsity level of the signal as an input to reconstruct the signals robustly in the presence of the noise.

The performance of all the 1-bit compressive algorithms in both the noiseless and the noisy scenarios were evaluated numerically in Chapter 5. From the simulations we found that:

- When the binary measurements vector $\mathbf{b}$ is noiseless, BIHT has less reconstruction error than BIHT-ℓ_2. However, as the level of the noise increases BIHT-ℓ_2 outperforms BIHT. The reason of this behaviour lies in the difference between ℓ_1-norm and ℓ_2-norm minimization applied in these two algorithms. The ℓ_1-norm minimization gives more accurate signal estimation than the ℓ_2-norm minimization when there is no noise in the binary measurements. In contrast, ℓ_2-norm minimization outperforms ℓ_1-norm minimization when there is noise in the binary measurements.

- In the scenario that the sparsity level of the signal is perfectly known, the performance of NARFPI is similar to the performance of AOP-f-ℓ_2 in different noisy scenarios. The ℓ_2-norm minimization in both NARFPI and AOP-f-ℓ_2 causes this similarity. In contrast, AOP-f outperforms NARFPI and AOP-f-ℓ_2 because of the ℓ_1-norm applied in AOP-f. Generally, we can conclude that in the noisy case and when the sparsity level of the signal is perfectly known, the reconstruction algorithms based on the ℓ_1-norm minimization have better performance than the reconstruction algorithms based on the ℓ_2-norm minimization.

- When the sparsity level of the signal deviates from its estimated value, NARFPI outperforms both AOP-f and AOP-f-ℓ_2 because NARFPI does not require a priori knowledge of the signal sparsity level. In other words, NARFPI is appealing in practical scenarios in which there is no perfect knowledge about the sparsity level. For instance, the sparsity level of the transformed images through wavelet transformation is not a deterministic value but has a calculable distribution with particular mean and variance. Therefore, in this scenario NARFPI outperforms AOP-f and AOP-f-ℓ_2.

6.1 Suggestion for future work

In this work, we proposed NARFPI which is an iterative algorithm mainly derived from RFPI. The cost function inside RFPI works based on the ℓ_2-norm. Therefore, NARFPI is generally an ℓ_2-norm based algorithm. This ℓ_2-norm in NARFPI is the reason of the similarity between performance of NARFPI and AOP-f-ℓ_2. As mentioned in the previous section, in the low-noise regime ℓ_1-norm based algorithms, e.g., AOP-f reconstruct the signal more accurately than the ones based on ℓ_2-norm. As a future work, one may apply a new cost function in NARFPI that is based on ℓ_1-norm. It is expected that the performance of the new resulting algorithm is identical to the performance of AOP-f when the sparsity level of the signal is known.

Appendices

Appendix A

Proof of Theorems in Chapter 2

A.1 Proof of Theorem 1

Proof. First, by assuming that $\mathbf{\Phi}$ satisfies the null space property, we prove the uniqueness of the solution. Let $\mathbf{z} \in \mathbb{C}^N$ be such that $\mathbf{\Phi z} = \mathbf{\Phi x}$, $\mathbf{z} \neq \mathbf{x}$. Then we have to show that $\|\mathbf{x}\|_1 < \|\mathbf{z}\|_1$, in other words, $\mathbf{x}$ is the sparsest possible solution. By assumption $\mathbf{v} = \mathbf{x} - \mathbf{z} \in \ker\{\mathbf{\Phi}\} \setminus \{0\}$. Let $T = \mathrm{supp}(\mathbf{x})$, $\mathbf{v}_T$ is the vector $\mathbf{v}$ spanned to entries with indices in T and $T^c = [N] \setminus T$ where $[N] = \{1, \dots N\}$. Then we have

$$\begin{aligned} \|\mathbf{x}\|_1 &= \|\mathbf{x} - \mathbf{z}_T + \mathbf{z}_T\|_1 \\ &\leq \|\mathbf{x} - \mathbf{z}_T\|_1 + \|\mathbf{z}_T\|_1 = \|\mathbf{v}_T\|_1 + \|\mathbf{z}_T\|_1 \\ &< \|\mathbf{v}_{T^c}\|_1 + \|\mathbf{z}_T\|_1 = \|-\mathbf{z}_{T^c}\|_1 + \|\mathbf{z}_T\|_1 = \|\mathbf{z}\|_1 . \end{aligned} \tag{A.1}$$

Therefore, $\mathbf{x}$ is the unique solution of (2.3).
In order to prove the converse of above, we take $\mathbf{v} = \mathbf{x} - \mathbf{z} \in \ker\{\mathbf{\Phi}\} \setminus \{0\}$ and $T \subset [N]$, $|T| = s$. By assumption, $\mathbf{v}_T$ is the unique solution of $\arg\min_{\mathbf{z}} \|\mathbf{z}\|_1$ and $\mathbf{\Phi z} = \mathbf{\Phi v}_T$, i.e.,

$$\mathbf{\Phi v}_T = \mathbf{\Phi z} \text{ and } \|\mathbf{v}_T\|_1 < \|\mathbf{z}\|_1 \ . \tag{A.2}$$

Also, we have

$$\mathbf{\Phi v}_T = -\mathbf{\Phi v}_{T^c} \ , \ (\mathbf{v}_T \neq \mathbf{v}_{T^c}) \ . \tag{A.3}$$

Hence, (A.2) and (A.3) give

$$\|\mathbf{v}_T\|_1 < \|\mathbf{v}_{T^c}\|_1 . \tag{A.4}$$

Therefore, $\mathbf{\Phi}$ satisfies the null space property. $\square$

A.2 Proof of Theorem 2

In the first part of this section, we introduce some theorems and lemmas helping us to prove Theorem 2.

Proposition 1. *For every matrix* $\mathbf{\Phi} \in \mathbb{C}^{M\times N}$*, restricted isometry constants are increasingly ordered, i.e.,*

$$\delta_1 \leq \delta_2 \leq \cdots \leq \delta_s \leq \cdots . \tag{A.5}$$

Proof. It is obvious that an s-sparse vector $\mathbf{x}$ can also be considered as a $s+1$-sparse vector. Therefore, we have

$$(1-\delta_{s+1}) \parallel \mathbf{x} \parallel_2^2 \leq (1-\delta_s) \parallel \mathbf{x} \parallel_2^2 \leq \parallel \mathbf{\Phi x} \parallel_2^2 \leq (1+\delta_s) \parallel \mathbf{x} \parallel_2^2 \leq (1+\delta_{s+1}) \parallel \mathbf{x} \parallel_2^2 \tag{A.6}$$

and, consequently,

$$\delta_s \leq \delta_{s+1}. \tag{A.7}$$

□

Theorem 6 (Rayleigh-Ritz, [22, Theorem 4.2.2])**.** *Let* $\mathbf{\Phi} \in \mathbb{C}^{N\times N}$ *be Hermitian, and let the eigenvalues of* $\mathbf{\Phi}$ *be ordered as*

$$\lambda_{\min} = \lambda_1 \leq \lambda_2 \leq \cdots \leq \lambda_{N-1} \leq \lambda_N = \lambda_{\max}\,. \tag{A.8}$$

Then

$$\lambda_1 \mathbf{x}^\dagger \mathbf{x} \leq \mathbf{x}^\dagger \mathbf{\Phi x} \leq \lambda_N \mathbf{x}^\dagger \mathbf{x} \quad \textit{for all} \quad \mathbf{x} \in \mathbb{C}^N \tag{A.9}$$

$$\lambda_{\max} = \lambda_N = \max_{\mathbf{x}\neq 0} \frac{\mathbf{x}^\dagger \mathbf{\Phi x}}{\mathbf{x}^\dagger \mathbf{x}} = \max_{\mathbf{x}^\dagger \mathbf{x}=1} \mathbf{x}^\dagger \mathbf{\Phi x} \tag{A.10}$$

$$\lambda_{\min} = \lambda_1 = \min_{\mathbf{x}\neq 0} \frac{\mathbf{x}^\dagger \mathbf{\Phi x}}{\mathbf{x}^\dagger \mathbf{x}} = \min_{\mathbf{x}^\dagger \mathbf{x}=1} \mathbf{x}^\dagger \mathbf{\Phi x}\,. \tag{A.11}$$

Lemma 2. *For every hermitian matrix* $\mathbf{\Phi} \in \mathbb{C}^{N\times N}$ *we have*

$$\max_{\|\mathbf{x}\|_2=1} \|\mathbf{\Phi x}\|_2 = \max_{\|\mathbf{x}\|_2=1} |\langle \mathbf{\Phi x}, \mathbf{x}\rangle|\,. \tag{A.12}$$

Proof. By applying Theorem 6 we obtain

$$\max_{\|\mathbf{x}\|_2=1} \|\mathbf{\Phi x}\|_2 = \max \sqrt{\frac{\|\mathbf{\Phi x}\|_2^2}{\|\mathbf{x}\|_2^2}} = \max \sqrt{\frac{\mathbf{x}^\dagger \mathbf{\Phi}^\dagger \mathbf{\Phi x}}{\mathbf{x}^\dagger \mathbf{x}}} = \sqrt{\lambda_{\max}\left(\mathbf{\Phi}^\dagger \mathbf{\Phi}\right)} = \sigma_{\max}\left(\mathbf{\Phi}\right), \tag{A.13}$$

where $\sigma_{\max}(\mathbf{\Phi})$ is the maximum singular value of $\mathbf{\Phi}$. In addition, $|\lambda\left(\mathbf{\Phi}\right)| = \sigma\left(\mathbf{\Phi}\right)$ since $\mathbf{\Phi}$ is hermitian. Therefore,

$$\sigma_{\max}\left(\mathbf{\Phi}\right) = |\lambda_{\max}\left(\mathbf{\Phi}\right)| = \max \left|\frac{\mathbf{x}^\dagger \mathbf{\Phi x}}{\mathbf{x}^\dagger \mathbf{x}}\right| = \max_{\|\mathbf{x}\|_2=1} |\langle \mathbf{\Phi x}, \mathbf{x}\rangle| . \tag{A.14}$$

□

Proposition 2 ([12, Proposition 2.5.c])**.** *Let* $\mathbf{\Phi} \in \mathbb{C}^{M\times N}$ *with restricted isometry constant* δ_s *and* $\mathbf{u}, \mathbf{v} \subset \mathbb{C}^N$ *with disjoint support, i.e., supp*$(\mathbf{u}) \cap$ *supp*$(\mathbf{v}) = \emptyset$ *and* $s =|$ *supp*$\left(\mathbf{u}\right) | + |$ *supp*$\left(\mathbf{v}\right) |$*. Then*

$$|\langle \mathbf{\Phi u}, \mathbf{\Phi v}\rangle| \leq \delta_s \|\mathbf{u}\|_2 \|\mathbf{v}\|_2 . \tag{A.15}$$

Proof. We can write (2.5) as

$$\left|\|\mathbf{\Phi x}\|_2^2 - \|\mathbf{x}\|_2^2\right| \leq \delta_s \|\mathbf{x}\|_2^2 \tag{A.16}$$

$$\begin{aligned} \frac{|\langle \mathbf{\Phi x}, \mathbf{\Phi x}\rangle - \langle \mathbf{x}, \mathbf{x}\rangle|}{\langle \mathbf{x}, \mathbf{x}\rangle} &= \frac{\left|\mathbf{x}^\dagger \mathbf{\Phi}^\dagger \mathbf{\Phi x} - \mathbf{x}^\dagger \mathbf{x}\right|}{\mathbf{x}^\dagger \mathbf{x}} = \frac{\left|\left\langle \mathbf{\Phi}^\dagger \mathbf{\Phi x}, \mathbf{x}\right\rangle - \langle \mathbf{x}, \mathbf{x}\rangle\right|}{\langle \mathbf{x}, \mathbf{x}\rangle} \\ &= \frac{\left|\left\langle \left(\mathbf{\Phi}^\dagger \mathbf{\Phi} - I\right) \mathbf{x}, \mathbf{x}\right\rangle\right|}{\langle \mathbf{x}, \mathbf{x}\rangle} \leq \delta_s. \end{aligned} \tag{A.17}$$

Therefore, from Lemma 2,

$$\max_{\|\mathbf{x}\|_2=1} \left|\left\langle \left(\mathbf{\Phi}^\dagger \mathbf{\Phi} - I\right) \mathbf{x}, \mathbf{x}\right\rangle\right| = \max_{\|\mathbf{x}\|_2=1} \left\|\left(\mathbf{\Phi}^\dagger \mathbf{\Phi} - I\right) \mathbf{x}\right\|_2 \leq \delta_s. \tag{A.18}$$

By definition $\operatorname{supp}\left(\mathbf{v}\right) = V$ and $\operatorname{supp}\left(\mathbf{u}\right) = U$ where $|V| + |U| = s$ and $V \cap U = \emptyset$. Let $\mathbf{0}_U$ and $\mathbf{0}_V$ be zero vectors with lengths $|U|$ and $|V|$, and $\left[\mathbf{0}_V^\dagger, \mathbf{u}_U^\dagger\right]^\dagger$ is a vector obtained by merging vectors $\mathbf{0}_V$ and $\mathbf{u}_U$. In addition, $\mathbf{\Phi}_{[:,S]}$ denotes a sub-matrix of $\mathbf{\Phi}$ spanned to columns in S where S is the combination of indices in V and U in order. Then, we can write

$$\begin{aligned}
\langle \mathbf{\Phi u}, \mathbf{\Phi v}\rangle &= \mathbf{v}_V^\dagger \mathbf{\Phi}_{[:,V]}^\dagger \mathbf{\Phi}_{[:,U]}\mathbf{u}_U = \left[\mathbf{v}_V^\dagger, \mathbf{0}_U^\dagger\right] \mathbf{\Phi}_{[:,S]}^\dagger \mathbf{\Phi}_{[:,S]} \left[\mathbf{0}_V^\dagger, \mathbf{u}_U^\dagger\right]^\dagger \\
&= \left[\mathbf{v}_V^\dagger, \mathbf{0}_U^\dagger\right] \mathbf{\Phi}_{[:,S]}^\dagger \mathbf{\Phi}_{[:,S]} \left[\mathbf{0}_V^\dagger, \mathbf{u}_U^\dagger\right]^\dagger - \underbrace{\left[\mathbf{v}_V^\dagger, \mathbf{0}_U^\dagger\right]\left[\mathbf{0}_V^\dagger, \mathbf{u}_U^\dagger\right]^\dagger}_{=0} \\
&= \underbrace{\left[\mathbf{v}_V^\dagger, \mathbf{0}_U^\dagger\right]}_{\mathbf{p}^\dagger} \underbrace{\left(\mathbf{\Phi}_{[:,S]}^\dagger \mathbf{\Phi}_{[:,S]} - I\right)}_{\mathbf{\Delta}} \underbrace{\left[\mathbf{0}_V^\dagger, \mathbf{u}_U^\dagger\right]^\dagger}_{\mathbf{q}}. \qquad (A.19)
\end{aligned}$$

From Cauchy-Schwartz inequality we have

$$\left|\mathbf{p}^\dagger \mathbf{\Delta q}\right| = |\langle \mathbf{\Delta q}, \mathbf{p}\rangle| \leq \|\mathbf{\Delta q}\|_2 \|\mathbf{p}\|_2 . \qquad (A.20)$$

Moreover, from (A.18) we know that

$$\frac{\|\mathbf{\Delta q}\|_2}{\|\mathbf{q}\|_2} \leq \max \frac{\|\mathbf{\Delta q}\|_2}{\|\mathbf{q}\|_2} \leq \delta_s. \qquad (A.21)$$

Hence,

$$\left|\mathbf{p}^\dagger \mathbf{\Delta q}\right| \leq \delta_s \|\mathbf{q}\|_2 \|\mathbf{p}\|_2 \Rightarrow |\langle \mathbf{\Phi u}, \mathbf{\Phi v}\rangle| \leq \delta_s \|\mathbf{u}\|_2 \|\mathbf{v}\|_2 \qquad (A.22)$$

□

Now we are ready to prove Theorem 2 by applying Propositions 1 and 2.

Proof. Take $\mathbf{v} \in \ker\{\mathbf{\Phi}\}$, let T_0 be the set of s largest modulus entries of $\mathbf{v}$ and $\mathbf{v}_{T_0}$ is a vector spanned to entries of $\mathbf{v}$ with indeces in T_0. Then $T_0^c = T_1 \cup T_2 \cup ...$ where T_i , for every $i > 0$, is the set containing s largest modulus entries of $\mathbf{v}_Q$, $Q = [N] \setminus \bigcup_{j=0}^{i-1} T_j$. Therefore, $\mathbf{\Phi}(\mathbf{v}_{T_0}) = -\mathbf{\Phi}\left(\mathbf{v}_{T_1} + \mathbf{v}_{T_2} + ...\right)$ and by using (2.5) and Proposition 1 we obtain

$$1 - \delta_{2s} \leq 1 - \delta_s \text{ and } (1 - \delta_{2\mathrm{s}}) \|\mathbf{v}_{T_0}\|_2^2 \leq \|\mathbf{\Phi}(\mathbf{v}_{T_0})\|_2^2 . \qquad (A.23)$$

Now we can write

$$\begin{aligned}
\|\mathbf{\Phi v}_{T_0}\|_2^2 &= \langle \mathbf{\Phi v}_{T_0}, \mathbf{\Phi v}_{T_0}\rangle = \langle \mathbf{\Phi v}_{T_0}, -\mathbf{\Phi}\left(\mathbf{v}_{T_1} + \mathbf{v}_{T_2} + ...\right)\rangle \\
&= \left\langle \mathbf{\Phi v}_{T_0}, \sum_{k\geq 1} -\mathbf{\Phi v}_{T_k} \right\rangle = \sum_{k\geq 1} \langle \mathbf{\Phi v}_{T_0}, -\mathbf{\Phi v}_{T_k}\rangle . \qquad (A.24)
\end{aligned}$$

Substituting (A.23) in (A.24) gives

$$\|\mathbf{v}_{T_0}\|_2^2 \leq \frac{1}{1-\delta_{2s}} \sum_{k\geq 1} \langle \mathbf{\Phi} \mathbf{v}_{T_0}, -\mathbf{\Phi} \mathbf{v}_{T_k} \rangle \tag{A.25}$$

and Proposition 2 yields

$$\langle \mathbf{\Phi} \mathbf{v}_{T_0}, -\mathbf{\Phi} \mathbf{v}_{T_k} \rangle \leq \delta_{2s} \|\mathbf{v}_{T_0}\|_2 \|\mathbf{v}_{T_k}\|_2 . \tag{A.26}$$

By substituting (A.26) in (A.25) we get

$$\|\mathbf{v}_{T_0}\|_2^2 \leq \frac{\delta_{2s}}{1-\delta_{2s}} \sum_{k\geq 1} \|\mathbf{v}_{T_0}\|_2 \|\mathbf{v}_{T_k}\|_2$$

$$\|\mathbf{v}_{T_0}\|_2 \leq \frac{\delta_{2s}}{1-\delta_{2s}} \sum_{k\geq 1} \|\mathbf{v}_{T_k}\|_2 \ . \tag{A.27}$$

The s entries of $\mathbf{v}_{T_k}$ do not exceed the s entries of $\mathbf{v}_{T_{k-1}}$ so

$$\forall\, j \in T_k \ \ |v_j| \leq \frac{1}{s} \sum_{l \in T_{k-1}} |v_l| = \frac{1}{s} \left\|\mathbf{v}_{T_{k-1}}\right\|_1$$

$$\begin{aligned} \|\mathbf{v}_{T_k}\|_2 &= \left(\sum_{j=T_k} |v_j|^{\,2} \right)^{1/2} \leq \left(s \cdot \left(\frac{1}{s} \left\|\mathbf{v}_{T_{k-1}}\right\|_1 \right)^2 \right)^{1/2} \\ &= \frac{1}{\sqrt{s}} \left\|\mathbf{v}_{T_{k-1}}\right\|_1 . \end{aligned} \tag{A.28}$$

Assume that $\mathbf{s}_0$ is a N-dimensional vector and

$$\mathbf{s}_0 = \begin{cases} s_j = 1 & j \in T_0 \\ s_j = 0 & j \notin T_0 \end{cases} . \tag{A.29}$$

By using Cauchy-Schwartz inequality we have

$$\|\mathbf{v}_{T_0}\|_1 = |\langle \mathbf{v}_{T_0}, \mathbf{s}_0 \rangle| \leq \|\mathbf{v}_{T_0}\|_2 \|\mathbf{s}_0\|_2 = \sqrt{s}\, \|\mathbf{v}_{T_0}\|_2 \ . \tag{A.30}$$

Applying (A.27) and (A.28) in (A.30) gives

$$\begin{aligned} &\|\mathbf{v}_{T_0}\|_1 \leq \sqrt{s}\, \|\mathbf{v}_{T_0}\|_2 \leq \frac{\delta_{2s}}{1-\delta_{2s}} \sum_{k\geq 1} \sqrt{s}\, \|\mathbf{v}_{T_k}\|_2 \leq \frac{\delta_{2s}}{1-\delta_{2s}} \sum_{k\geq 1} \left\|\mathbf{v}_{T_{k-1}}\right\|_1 \\ &= \frac{\delta_{2s}}{1-\delta_{2s}} \left(\|\mathbf{v}_{T_0}\|_1 + \sum_{k\geq 1} \|\mathbf{v}_{T_k}\|_1 \right) \leq \frac{\delta_{2s}}{1-\delta_{2s}} (\|\mathbf{v}_{T_0}\|_1 + \left\|\mathbf{v}_{T_0^c}\right\|_1) \end{aligned} \tag{A.31}$$

Now if $\delta_{2s} < 1/3$ or $\frac{\delta_{2s}}{1-\delta_{2s}} < 1/2$, then

$$\|\mathbf{v}_{T_0}\|_1 \leq \frac{\delta_{2s}}{1-\delta_{2s}}(\|\mathbf{v}_{T_0}\|_1 + \left\|\mathbf{v}_{T_0^c}\right\|_1) < \frac{1}{2}(\|\mathbf{v}_{T_0}\|_1 + \left\|\mathbf{v}_{T_0^c}\right\|_1) . \tag{A.32}$$

Therefore, we have that

$$\|\mathbf{v}_{T_0}\|_1 < \left\|\mathbf{v}_{T_0^c}\right\|_1 \tag{A.33}$$

so the null space property follows. □

A.3 Proof of Theorem 3

First we introduce some intermediate theorems and definitions which help us to prove Theorem 3.

Proposition 3. *If $\mathbf{\Phi} \in \mathbb{C}^{M\times N}$satisfies RIP with Restricted Isometry Constant δ_s then for all $T \subset [N]$ and $\mid T \mid\leq s$ we have*

$$1-\delta_s \leq \lambda_{\min}\left(\mathbf{\Phi}^{\dagger}_{[:,T]}\mathbf{\Phi}_{[:,T]}\right) \leq \lambda_{\max}\left(\mathbf{\Phi}^{\dagger}_{[:,T]}\mathbf{\Phi}_{[:,T]}\right) \leq 1+\delta_s \tag{A.34}$$

and

$$\sqrt{1-\delta_s} \leq \sigma_{\min}\left(\mathbf{\Phi}_{[:,T]}\right) \leq \sigma_{\max}\left(\mathbf{\Phi}_{[:,T]}\right) \leq \sqrt{1+\delta_s}. \tag{A.35}$$

Proof. We know that

$$(1-\delta_s)\|\mathbf{x}\|_2^2 \leq \|\mathbf{\Phi x}\|_2^2 \leq (1+\delta_s)\|\mathbf{x}\|_2^2 \quad \text{for every } s\text{-sparse } \mathbf{x}\,.$$

Then we can write

$$\left|\|\mathbf{\Phi x}\|_2^2 - \|\mathbf{x}\|_2^2\right| \leq \delta_s \|\mathbf{x}\|_2^2\ . \tag{A.36}$$

By applying $\|\mathbf{x}\|_2^2 = \langle \mathbf{x},\mathbf{x}\rangle = \mathbf{x}^{\dagger}\mathbf{x}$ we can write the left-hand side of (A.36) as

$$\begin{aligned}\left|\|\mathbf{\Phi x}\|_2^2 - \|\mathbf{x}\|_2^2\right| &= |\langle \mathbf{\Phi x},\mathbf{\Phi x}\rangle - \langle \mathbf{x},\mathbf{x}\rangle| = \left|\mathbf{x}^{\dagger}\mathbf{\Phi}^{\dagger}\mathbf{\Phi x} - \langle \mathbf{x},\mathbf{x}\rangle\right| \\ &= \left|\left\langle \mathbf{\Phi}^{\dagger}\mathbf{\Phi x},\mathbf{x}\right\rangle - \langle \mathbf{x},\mathbf{x}\rangle\right| = \left|\left\langle \mathbf{\Phi}^{\dagger}\mathbf{\Phi x}-\mathbf{x},\mathbf{x}\right\rangle\right| \\ &= \left|\left\langle \left(\mathbf{\Phi}^{\dagger}\mathbf{\Phi}-\boldsymbol{I}\right)\mathbf{x},\mathbf{x}\right\rangle\right| = \left|\mathbf{x}^{\dagger}\left(\mathbf{\Phi}^{\dagger}\mathbf{\Phi}-\boldsymbol{I}\right)\mathbf{x}\right|. \end{aligned} \tag{A.37}$$

Substituting (A.37) in (A.36) yields

$$\left|\mathbf{x}^{\dagger}\left(\mathbf{\Phi}^{\dagger}\mathbf{\Phi}-\boldsymbol{I}\right)\mathbf{x}\right| \leq \delta_s\mathbf{x}^{\dagger}\mathbf{x}\,.$$

Since $\mathbf{x}$ is s-sparse we obtain

$$\mathbf{x}_T^\dagger \mathbf{x}_T = \mathbf{x}^\dagger \mathbf{x}. \tag{A.38}$$

Therefore,

$$\mathbf{x}_T^\dagger \left(\mathbf{\Phi}_{[:,T]}^\dagger \mathbf{\Phi}_{[:,T]} - \boldsymbol{I} \right) \mathbf{x}_T = \mathbf{x}^\dagger \left(\mathbf{\Phi}^\dagger \mathbf{\Phi} - \boldsymbol{I} \right) \mathbf{x}\,, \tag{A.39}$$

where $T = \operatorname{supp}(\mathbf{x})$. From (A.38), (A.39) and Theorem 6 we have (for all s-sparse $\mathbf{x}$ with support T)

$$\lambda_{\min} \left(\mathbf{\Phi}_{[:,T]}^\dagger \mathbf{\Phi}_{[:,T]} - \boldsymbol{I} \right) \mathbf{x}^\dagger \mathbf{x} \le \mathbf{x}^\dagger \left(\mathbf{\Phi}^\dagger \mathbf{\Phi} - \boldsymbol{I} \right) \mathbf{x} \le \lambda_{\max} \left(\mathbf{\Phi}_{[:,T]}^\dagger \mathbf{\Phi}_{[:,T]} - \boldsymbol{I} \right) \mathbf{x}^\dagger \mathbf{x}$$

$$\left| \mathbf{x}^\dagger \left(\mathbf{\Phi}^\dagger \mathbf{\Phi} - \boldsymbol{I} \right) \mathbf{x} \right| \le \max \left\{ \lambda_{\max} \left(\mathbf{\Phi}_{[:,T]}^\dagger \mathbf{\Phi}_{[:,T]} - \boldsymbol{I} \right) \mathbf{x}^\dagger \mathbf{x}, -\lambda_{\min} \left(\mathbf{\Phi}_{[:,T]}^\dagger \mathbf{\Phi}_{[:,T]} - \boldsymbol{I} \right) \mathbf{x}^\dagger \mathbf{x} \right\}. \tag{A.40}$$

In other words, (A.40) implies that if $0 < \lambda_{\min} \left(\mathbf{\Phi}_{[:,T]}^\dagger \mathbf{\Phi}_{[:,T]} - \boldsymbol{I} \right) \mathbf{x}^\dagger \mathbf{x}$ then

$$\left| \mathbf{x}^\dagger \left(\mathbf{\Phi}^\dagger \mathbf{\Phi} - \boldsymbol{I} \right) \mathbf{x} \right| \le \lambda_{\max} \left(\mathbf{\Phi}_{[:,T]}^\dagger \mathbf{\Phi}_{[:,T]} - \boldsymbol{I} \right) \mathbf{x}^\dagger \mathbf{x}, \tag{A.41}$$

but in the case that $0 > \lambda_{\min} \left(\mathbf{\Phi}_{[:,T]}^\dagger \mathbf{\Phi}_{[:,T]} - \boldsymbol{I} \right) \mathbf{x}^\dagger \mathbf{x}$ then simply $\left| \mathbf{x}^\dagger \left(\mathbf{\Phi}^\dagger \mathbf{\Phi} - \boldsymbol{I} \right) \mathbf{x} \right| \le \max \left\{ \left| \lambda_{\max} \left(\mathbf{\Phi}_{[:,T]}^\dagger \mathbf{\Phi}_{[:,T]} - \boldsymbol{I} \right) \mathbf{x}^\dagger \mathbf{x} \right| , \left| \lambda_{\min} \left(\mathbf{\Phi}_{[:,T]}^\dagger \mathbf{\Phi}_{[:,T]} - \boldsymbol{I} \right) \mathbf{x}^\dagger \mathbf{x} \right| \right\}$. Comparing (2.5) and (A.40) gives

$$\delta_s = \max \left\{ \lambda_{\max} \left(\mathbf{\Phi}_{[:,T]}^\dagger \mathbf{\Phi}_{[:,T]} - \boldsymbol{I} \right) , -\lambda_{\min} \left(\mathbf{\Phi}_{[:,T]}^\dagger \mathbf{\Phi}_{[:,T]} - \boldsymbol{I} \right) \right\}$$

$$\delta_s = \max \left\{ \lambda_{\max} \left(\mathbf{\Phi}_{[:,T]}^\dagger \mathbf{\Phi}_{[:,T]} \right) - 1 \,, 1 - \lambda_{\min} \left(\mathbf{\Phi}_{[:,T]}^\dagger \mathbf{\Phi}_{[:,T]} \right) \right\}$$

or

$$1 - \delta_s \le \lambda_{\min} \left(\mathbf{\Phi}_{[:,T]}^\dagger \mathbf{\Phi}_{[:,T]} \right) \le \lambda_{\max} \left(\mathbf{\Phi}_{[:,T]}^\dagger \mathbf{\Phi}_{[:,T]} \right) \le 1 + \delta_s\,. \tag{A.42}$$

□

Definition 6 (Lipschitz condition, [23, page 46]). Let $f(\mathbf{x})$ be defined on an interval I and suppose we can find a positive constant α such that

$$|f(\mathbf{x}_1) - f(\mathbf{x}_2)| \le \alpha \left\| \mathbf{x}_1 - \mathbf{x}_2 \right\|_2 \tag{A.43}$$

for all $\mathbf{x}_1$, $\mathbf{x}_2 \in I$. Then f is said to satisfy a Lipschitz condition with Lipschitz constant α.

Example 1. The maximum and minimum singular values of any $\mathbf{\Phi} \in \mathbb{C}^{M \times N}$ are Lipschitz functions with Lipschitz constant 1.

Proof. From Theorem 6

$$\max \frac{\mathbf{x}^\dagger \mathbf{\Phi}^\dagger \mathbf{\Phi} \mathbf{x}}{\mathbf{x}^\dagger \mathbf{x}} = \max \frac{\|\mathbf{\Phi x}\|_2^2}{\|\mathbf{x}\|_2^2} = \lambda_{\max}\left(\mathbf{\Phi}^\dagger \mathbf{\Phi}\right) = \sigma_{\max}^2\left(\mathbf{\Phi}\right) \tag{A.44}$$

$$\min \frac{\mathbf{x}^\dagger \mathbf{\Phi}^\dagger \mathbf{\Phi} \mathbf{x}}{\mathbf{x}^\dagger \mathbf{x}} = \min \frac{\|\mathbf{\Phi x}\|_2^2}{\|\mathbf{x}\|_2^2} = \lambda_{\min}\left(\mathbf{\Phi}^\dagger \mathbf{\Phi}\right) = \sigma_{\min}^2\left(\mathbf{\Phi}\right). \tag{A.45}$$

By definition we have

$$\|\mathbf{\Phi}\|_{\mathrm{F}} = \sqrt{\mathrm{tr}\left(\mathbf{\Phi}^\dagger \mathbf{\Phi}\right)} = \sqrt{\sum_i \sigma_i^2\left(\mathbf{\Phi}\right)} \tag{A.46}$$

where $\sigma_i\left(\mathbf{\Phi}\right)$ is i-th singular value of $\mathbf{\Phi}$ and $\|\cdot\|_{\mathrm{F}}$ denotes Frobenius-norm. Therefore

$$\sigma_{\min}\left(\mathbf{\Phi}\right) \leq \sigma_{\max}\left(\mathbf{\Phi}\right) \leq \|\mathbf{\Phi}\|_F. \tag{A.47}$$

We know from Triangular inequality that

$$\text{for any } \mathbf{\Phi}, \mathbf{\Xi} \in \mathbb{C}^{M \times N} \quad \|\mathbf{\Phi x}\|_2 \leq \|\mathbf{\Xi x}\|_2 + \|\left(\mathbf{\Phi} - \mathbf{\Xi}\right)\mathbf{x}\|_2. \tag{A.48}$$

From (A.48) we obtain

$$\max \|\mathbf{\Phi x}\|_2 \leq \max \|\mathbf{\Xi x}\|_2 + \max \|\left(\mathbf{\Phi} - \mathbf{\Xi}\right)\mathbf{x}\|_2 \tag{A.49}$$

and

$$\min \|\mathbf{\Phi x}\|_2 \leq \min \|\mathbf{\Xi x}\|_2 + \min \|\left(\mathbf{\Phi} - \mathbf{\Xi}\right)\mathbf{x}\|_2. \tag{A.50}$$

Therefore, by substituting (A.44) and (A.45) in (A.49) and (A.50) we obtain

$$\sigma_{\max}\left(\mathbf{\Phi}\right) \leq \sigma_{\max}\left(\mathbf{\Xi}\right) + \sigma_{\max}\left(\mathbf{\Phi} - \mathbf{\Xi}\right) \tag{A.51}$$

$$\sigma_{\min}\left(\mathbf{\Phi}\right) \leq \sigma_{\min}\left(\mathbf{\Xi}\right) + \sigma_{\min}\left(\mathbf{\Phi} - \mathbf{\Xi}\right). \tag{A.52}$$

In addition, from (A.47) we have

$$\sigma_{\max}\left(\mathbf{\Phi}\right) - \sigma_{\max}\left(\mathbf{\Xi}\right) \leq \sigma_{\max}\left(\mathbf{\Phi} - \mathbf{\Xi}\right) \leq \|\mathbf{\Phi} - \mathbf{\Xi}\|_{\mathrm{F}} \tag{A.53}$$

$$\sigma_{\min}\left(\mathbf{\Phi}\right) - \sigma_{\min}\left(\mathbf{\Xi}\right) \leq \sigma_{\min}\left(\mathbf{\Phi} - \mathbf{\Xi}\right) \leq \|\mathbf{\Phi} - \mathbf{\Xi}\|_{\mathrm{F}}. \tag{A.54}$$

Since we can interchange $\mathbf{\Phi}$ and $\mathbf{\Xi}$, we get

$$|\sigma_{\max}(\mathbf{\Phi}) - \sigma_{\max}(\mathbf{\Xi})| \leq \|\mathbf{\Phi} - \mathbf{\Xi}\|_{\mathrm{F}}$$

$$|\sigma_{\min}(\mathbf{\Phi}) - \sigma_{\min}(\mathbf{\Xi})| \leq \|\mathbf{\Phi} - \mathbf{\Xi}\|_{\mathrm{F}}. \tag{A.55}$$

Therefore, $\sigma_{\max}(\cdot)$ and $\sigma_{\min}(\cdot)$ satisfy Lipschitz condition with constant $\alpha = 1$. □

Theorem 7 ([24, Lemma 2.2])**.** *Let* $\mathbf{x}$ *be a* N*-dimensional vector of unit variance, independent Gaussian variables, if* $f : \mathbb{R}^N \to \mathbb{R}$ *is Lipschitz function with Lipschitz constant* α *then for all* $t > 0$

$$\mathbb{P}(f(\mathbf{x}) - \mathbb{E}(f(\mathbf{x})) > t) \leq e^{-t^2/2\alpha^2}. \tag{A.56}$$

Theorem 8 (Gordon's theorem, [25, Theorem 5.32])**.** *Let* $\mathbf{\Phi}$ *be an* M *by* N *array of i.i.d* $\mathcal{N}(0,1)$ *then*

$$\mathbb{E}(\sigma_{\min}(\mathbf{\Phi})) \geq \sqrt{M} - \sqrt{N} \text{ and } \mathbb{E}(\sigma_{\max}(\mathbf{\Phi})) \leq \sqrt{M} + \sqrt{N}. \tag{A.57}$$

Proposition 4. *For any matrix* $\mathbf{\Phi} \in \mathbb{C}^{M \times N}$ *with i.i.d* $\mathcal{N}(0,1)$ *modulus entries,*

$$\mathbb{P}\left(\sigma_{\min}(\mathbf{\Phi}) < \sqrt{M} - \sqrt{N} - t\right) \leq e^{-t^2/2}$$

$$\mathbb{P}\left(\sigma_{\max}(\mathbf{\Phi}) > \sqrt{M} + \sqrt{N} + t\right) \leq e^{-t^2/2}. \tag{A.58}$$

Proof. From Example 1 we know that $\sigma_{\min}(\mathbf{\Phi})$ and $\sigma_{\max}(\mathbf{\Phi})$ are Lipschitz with constant 1. Therefore, applying Theorem 7 gives

$$\mathbb{P}(\mathbb{E}(\sigma_{\min}(\mathbf{\Phi})) - \sigma_{\min}(\mathbf{\Phi}) > t) \leq e^{-t^2/2}$$

$$\mathbb{P}(\sigma_{\max}(\mathbf{\Phi}) - \mathbb{E}(\sigma_{\max}(\mathbf{\Phi})) > t) \leq e^{-t^2/2}. \tag{A.59}$$

From Theorem 8

$$\sqrt{M} - \sqrt{N} \leq \mathbb{E}(\sigma_{\min}(\mathbf{\Phi})) \text{ and } \sqrt{M} + \sqrt{N} \geq \mathbb{E}(\sigma_{\max}(\mathbf{\Phi})). \tag{A.60}$$

Therefore,

$$\mathbb{P}\left(\sigma_{\min}(\mathbf{\Phi}) < \sqrt{M} - \sqrt{N} - t\right) \leq \mathbb{P}\left(\sigma_{\min}(\mathbf{\Phi}) < \mathbb{E}\left(\sigma_{\min}(\mathbf{\Phi})\right) - t\right) \leq e^{-t^2/2}$$

$$\mathbb{P}\left(\sigma_{\max}(\mathbf{\Phi}) > \sqrt{M} + \sqrt{N} + t\right) \leq \mathbb{P}\left(\sigma_{\max}(\mathbf{\Phi}) > \mathbb{E}\left(\sigma_{\max}(\mathbf{\Phi})\right) + t\right) \leq e^{-t^2/2}. \tag{A.61}$$

□

Now by applying Propositions 3 and 4 we prove Theorem 3.

Proof. Let $T \subset [N]$ and $|T| \leq 2s$. We are interested to find the case that Proposition 3 holds for $\mathbf{\Phi}$ with high probability. In other words, $\mathbf{\Phi}$ will satisfy RIP with high probability when

$$\mathbb{P}\left(\sigma_{\min}(\mathbf{\Phi}_{[:,T]}) < \sqrt{1 - \delta_{2s}}\right) \tag{A.62}$$

and

$$\mathbb{P}\left(\sigma_{\max}(\mathbf{\Phi}_{[:,T]}) > \sqrt{1 + \delta_{2s}}\right) \tag{A.63}$$

are small enough.
By using Proposition 4 and dividing left side statement by $\sqrt{M}$, for every T we get

$$\mathbb{P}\left(\sigma_{\min}(\mathbf{\Phi}_{[:,T]}) < 1 - \sqrt{|T|/M} - k\right) \leq e^{-Mk^2/2} \tag{A.64}$$

$$\mathbb{P}\left(\sigma_{\max}(\mathbf{\Phi}_{[:,T]}) > 1 + \sqrt{|T|/M} + k\right) \leq e^{-Mk^2/2} \tag{A.65}$$

where $k = t/\sqrt{M}$. Since $\sigma_{\max}(\mathbf{\Phi}_{[:,T]})$ and $\sigma_{\min}(\mathbf{\Phi}_{[:,T]})$ increase by decreasing $\mid T \mid$, we have

$$\mathbb{P}_{T:|T|\leq 2s}\left(\sigma_{\max}\left(\mathbf{\Phi}_{[:,T]}\right) > \sqrt{1 + \delta_{2s}}\right) = \mathbb{P}_{T:|T|=2s}\left(\sigma_{\max}\left(\mathbf{\Phi}_{[:,T]}\right) > \sqrt{1 + \delta_{2s}}\right) \tag{A.66}$$

and applying (A.65) over all Ts satisfying $|T| = 2s$ gives

$$\begin{aligned}\mathbb{P}_{T:|T|=2s}\left(\sigma_{\max}\left(\mathbf{\Phi}_{[:,T]}\right) > 1 + \sqrt{2s/M} + k\right) &\leq \#\left\{T : |T| = 2s\right\}.e^{-Mk^2/2} \\ &\leq \binom{N}{2s}.e^{-Mk^2/2}.\end{aligned} \tag{A.67}$$

We use following approximation

$$\binom{N}{2s} \approx \left(\frac{N}{2s}\right)^{2s} = e^{2s\log(N/2s)}. \tag{A.68}$$

Substituting above approximation in (A.67) gives

$$\underset{T:|T|\leq 2s}{\mathbb{P}}\left(\sigma_{\max}\left(\mathbf{\Phi}_{[:,T]}\right) > 1 + \sqrt{2s/M} + k\right) < e^{2s\log(N/2s)}.e^{-Mk^2/2}. \tag{A.69}$$

Therefore we have

$$\underset{T:|T|\leq 2s}{\mathbb{P}}\left(\sigma_{\max}\left(\mathbf{\Phi}_{[:,T]}\right) < 1 + \sqrt{2s/M} + k\right) \geq 1 - e^{2s\log(N/2s)}.e^{-Mk^2/2}. \tag{A.70}$$

Null space property holds when the conditions below are fulfilled. Firstly,

$$1 + \sqrt{2s/M} + k < \sqrt{1 + \delta_{2s}}, \tag{A.71}$$

where $\delta_{2s} < 1/3$. In addition,

$$2s(\log(N/2s)) - Mk^2/2 \leq 0, \tag{A.72}$$

which implies that the probability is always between zero and one. From (A.71) we have

$$0 < k < 0.15 - \sqrt{2s/M} \tag{A.73}$$

On the other hand, from (A.72) we have

$$\frac{4s(\log(N/s) - \log(2))}{k^2} = \frac{4s(\log(N/s) - 2.77s)}{k^2} \leq M. \tag{A.74}$$

Therefore, by choosing $4s\log(N/s)/k^2 \leq M$, (A.74) holds. For $\sigma_{\min}(\mathbf{\Phi})$ the proof is the same as above. In the case that (A.73) and (A.74) hold we have

$$\underset{T:|T|\leq 2s}{\mathbb{P}}\left(\sigma_{\max}\left(\mathbf{\Phi}_{[:,T]}\right) < \sqrt{1 + \delta_{2s}}\right) \geq 1 - e^{2s\log(N/2s)}.e^{-Mk^2/2} \tag{A.75}$$

Similarly, for $\sigma_{min}(\mathbf{\Phi})$ we have

$$\underset{T:|T|\leq 2s}{\mathbb{P}}\left(\sigma_{\min}\left(\mathbf{\Phi}_{[:,T]}\right) > \sqrt{1 - \delta_{2s}}\right) \geq 1 - e^{2s\log(N/2s)}.e^{-Mk^2/2} \tag{A.76}$$

Now if we name (A.75) $\mathbb{P}(A)$ and (A.76) $\mathbb{P}(B)$ then we are interested to find $\mathbb{P}(A \cap B)$ and from basic probability theory we know

$$\mathbb{P}(A \cap B) \geq \mathbb{P}(A) + \mathbb{P}(B) - 1. \tag{A.77}$$

Therefore, from (A.75), (A.76) and (A.77) we obtain

$$\begin{aligned}\underset{T:|T|\leq 2s}{\mathbb{P}}\left(\sqrt{1 - \delta_{2s}} < \sigma_{\min}\left(\mathbf{\Phi}_{[:,T]}\right) < \sigma_{\min}\left(\mathbf{\Phi}_{[:,T]}\right) < \sqrt{1 + \delta_{2s}}\right)& \\ \geq 1 - 2e^{2s\log(N/2s)}.e^{-Mk^2/2}&\end{aligned} \tag{A.78}$$

□

A.4 Proof of Theorem 4

We need to prove some intermediate theorems and lemmas which help us to prove Theorem 4. The main part of this section is derived from [16].

Lemma 3 ([16, Theorem 7.2])**.** *Assume that* $\mathbf{x} = [X_1, X_2, \ldots, X_N]$ *where each* $X_i \sim \mathrm{Sub}\left(c^2\right)$ *is independent. Then for any* $\mathbf{a} \in \mathbb{R}^N$, $\langle \mathbf{x}, \mathbf{a} \rangle \sim \mathrm{Sub}\left(\mathrm{c}^2 \|\mathbf{a}\|_2^2\right)$. *Similarly, if each* $X_i \sim \mathrm{SSub}\left(\sigma^2\right)$, *then for any* $\mathbf{a} \in \mathbb{R}^N$, $\langle \mathbf{x}, \mathbf{a} \rangle \sim \mathrm{SSub}\left(\sigma^2 \|\mathbf{a}\|_2^2\right)$.

Proof. Since X_i are i.i.d, factorization gives

$$\begin{aligned}
\mathbb{E}\left(\exp\left(t\sum_{i=1}^{N} a_i X_i\right)\right) &= \mathbb{E}\left(\prod_{i=1}^{N} \exp\left(t a_i X_i\right)\right) \\
&= \prod_{i=1}^{N} \mathbb{E}\left(\exp\left(t a_i X_i\right)\right) \\
&\leq \prod_{i=1}^{N} \exp\left(c^2 \left(t a_i\right)/2\right) \\
&= \exp\left(\left(\sum_{i=1}^{N} a_i^2\right) c^2 t^2/2\right). \qquad \text{(A.79)}
\end{aligned}$$

If the X_i are strictly sub-Gaussian, then setting $c^2 = \sigma^2$ gives $\mathbb{E}\left(\langle \mathbf{x}, \mathbf{a} \rangle^2\right) = \sigma^2 \|\mathbf{a}\|_2^2$. ☐

Lemma 4 (Markov's Inequality)**.** *For any random variable* $X > 0$ *and* $t > 0$,

$$\mathbb{P}\left(X \geq t\right) \leq \frac{\mathbb{E}\left(X\right)}{t}. \qquad \text{(A.80)}$$

Proof. By noting that $f\left(x\right)$ is the p.d.f. for X

$$\mathbb{E}\left(X\right) = \int_0^\infty x f\left(x\right) dx \geq \int_t^\infty x f\left(x\right) dx \geq \int_t^\infty t f\left(x\right) dx = t\mathbb{P}\left(X \geq t\right). \qquad \text{(A.81)}$$

☐

Lemma 5 ([16, Lemma 7.4])**.** *Let* $X \sim \mathrm{Sub}\left(c^2\right)$. *Then*

$$\mathbb{E}\left(\exp\left(\lambda X^2/2c^2\right)\right) \leq \frac{1}{\sqrt{1-\lambda}} \quad \text{for any } \lambda \in [0, 1). \qquad \text{(A.82)}$$

Proof. If $\lambda = 0$, then the lemma simply holds. Now suppose that $\lambda \in (0, 1)$. Since X is sub-Gaussian, we have

$$\int_{-\infty}^{\infty} \exp(tx) f(x)\, dx \leq \exp\left(c^2 t^2/2\right) \text{ for any } t \in \mathbb{R}. \tag{A.83}$$

By multiplying both sides by $\exp(-c^2t^2/2\lambda)$ we get

$$\int_{-\infty}^{\infty} \exp\left(tx - c^2t^2/2\lambda\right) f(x)\, dx \leq \exp\left(c^2t^2(\lambda - 1)/2\right). \tag{A.84}$$

Now integrating both sides with respect to t gives

$$\int_{-\infty}^{\infty} \left(\int_{-\infty}^{\infty} \exp\left(tx - c^2t^2/2\lambda\right) dt\right) f(x)\, dx \leq \int_{-\infty}^{\infty} \exp\left(c^2t^2(\lambda - 1)/2\right) dt$$

$$\frac{1}{c}\sqrt{2\pi\lambda} \int_{-\infty}^{\infty} \exp\left(\lambda x^2/2c^2\right) f(x)\, dx \leq \frac{1}{c}\sqrt{\frac{2\pi\lambda}{1-\lambda}}. \tag{A.85}$$

□

Theorem 9 ([16, Theorem 7.2])**.** *Suppose that* $\mathbf{x} = [X_1, X_2, \ldots, X_N]$*, where each* X_i *is i.i.d. with* $X_i \sim \mathrm{Sub}(c^2)$ *and* $\mathbb{E}(X_i^2) = \sigma^2$*. Then*

$$\mathbb{E}\left(\|\mathbf{x}\|_2^2\right) = M\sigma^2. \tag{A.86}$$

In addition, for any $\alpha \in (0, 1)$ *and for any* $\beta \in [c^2/\sigma^2, \beta_{\max}]$*, there exists a constant* $\mu \geq 4$ *depending only on* $\beta_{\max}$ *and the ratio* σ^2/c^2 *such that*

$$\mathbb{P}\left(\|\mathbf{x}\|_2^2 \leq \alpha M\sigma^2\right) \leq \exp\left(-M(1-\alpha)^2/\mu\right) \tag{A.87}$$

and

$$\mathbb{P}\left(\|\mathbf{x}\|_2^2 \geq \beta M\sigma^2\right) \leq \exp\left(-M(\beta-1)^2/\mu\right). \tag{A.88}$$

Proof. Since X_i are independent,

$$\mathbb{E}\left(\|\mathbf{x}\|_2^2\right) = \sum_{i=1}^{M} \mathbb{E}\left(X_i^2\right) = \sum_{i=1}^{M} \sigma^2 = M\sigma^2, \tag{A.89}$$

therefore, (A.86) holds. From Lemma 4 we have

$$\begin{aligned} \mathbb{P}\left(\|\mathbf{x}\|_2^2 \geq \beta M\sigma^2\right) &= \mathbb{P}\left(\exp\left(\lambda\|\mathbf{x}\|_2^2\right) \geq \exp\left(\lambda\beta M\sigma^2\right)\right) \\ &\leq \frac{\mathbb{E}\left(\exp\left(\lambda\|\mathbf{x}\|_2^2\right)\right)}{\exp(\lambda\beta M\sigma^2)} = \frac{\prod_{i=1}^{M}\mathbb{E}\left(\exp(\lambda X_i^2)\right)}{\exp(\lambda\beta M\sigma^2)}. \end{aligned} \tag{A.90}$$

From Lemma 5 we have

$$\mathbb{E}\left(\exp\left(\lambda X_i^2\right)\right) = \mathbb{E}\left(\exp\left(2c^2\lambda X_i^2/2c^2\right)\right) \leq \frac{1}{\sqrt{1-2c^2\lambda}}. \tag{A.91}$$

Therefore,

$$\prod_{i=1}^{M}\mathbb{E}\left(\exp\left(\lambda X_i^2\right)\right) \leq \left(\frac{1}{1-2c^2\lambda}\right)^{M/2} \tag{A.92}$$

and hence

$$\mathbb{P}\left(\|\mathbf{x}\|_2^2 \geq \beta M\sigma^2\right) \leq \left(\frac{\exp\left(-2\lambda\beta\sigma^2\right)}{1-2c^2\lambda}\right)^{M/2}. \tag{A.93}$$

The optimal λ, which can be found by setting the derivative to zero and solving for λ, is

$$\lambda = \frac{\beta\sigma^2 - c^2}{2c^2\sigma^2\left(1+\beta\right)}. \tag{A.94}$$

Substituting the optimal λ in (A.93) gives

$$\mathbb{P}\left(\|\mathbf{x}\|_2^2 \geq \beta M\sigma^2\right) \leq \left(\beta\frac{\sigma^2}{c^2}\exp\left(1-\beta\frac{\sigma^2}{c^2}\right)\right)^{M/2}. \tag{A.95}$$

Similarly for α we have

$$\mathbb{P}\left(\|\mathbf{x}\|_2^2 \geq \alpha M\sigma^2\right) \leq \left(\alpha\frac{\sigma^2}{c^2}\exp\left(1-\alpha\frac{\sigma^2}{c^2}\right)\right)^{M/2}. \tag{A.96}$$

If we define

$$\mu = \max\left(4, 2\frac{\left(\beta_{\max}\sigma^2/c-1\right)^2}{\left(\beta_{\max}\sigma^2/c-1\right)-\log\left(\beta_{\max}\sigma^2/c\right)}\right) \tag{A.97}$$

then we have that for any $\gamma \in [0, \beta_{\max}\sigma^2/c]$ we have the bound

$$\log\left(\gamma\right) \leq \left(\gamma-1\right) - \frac{2\left(\gamma-1\right)^2}{\mu}, \tag{A.98}$$

and therefore

$$\gamma \leq \exp\left(\left(\gamma-1\right) - \frac{2\left(\gamma-1\right)^2}{\mu}\right). \tag{A.99}$$

By setting $\gamma = \alpha\sigma^2/c^2$, we can obtain (A.87). In the same way, setting $\gamma = \beta\sigma^2/c^2$ gives (A.88). $\square$

Corollary 1 ([16, Corollary 7.1])**.** *Suppose that* $\mathbf{x} = [X_1, X_2, \ldots, X_N]$*, where each* X_i *is i.i.d. with* $X_i \sim \mathrm{SSub}(\sigma^2)$*. Then*

$$\mathbb{E}\left(\|\mathbf{x}\|_2^2\right) = M\sigma^2 \tag{A.100}$$

and for any $\epsilon > 0$*,*

$$\mathbb{P}\left(\mid \|\mathbf{x}\|_2^2 - M\sigma^2 \mid \geq \epsilon M\sigma^2\right) \leq 2\exp\left(-\frac{M\epsilon^2}{\mu}\right) \tag{A.101}$$

with $\mu = 2/(1-\log(2)) \approx 6.52$*.*

Proof. Since $X_i \sim \mathrm{SSub}(\sigma^2)$, we have that $X_i \sim \mathrm{Sub}(\sigma^2)$ and $\mathbb{E}(X_i^2) = \sigma^2$ and by setting $\alpha = 1-\epsilon$ and $\beta = 1+\epsilon$ in Theorem 9 we obtain (A.101) with $\beta_{\max} = 2$. By substituting $c^2 = \sigma^2$ and $\beta_{\max} = 2$ in (A.97) we obtain $\mu = 2/(1-\log(2))$. □

Corollary 2 ([16, Corollary 7.2])**.** *Suppose that* $\mathbf{\Phi} \in \mathbb{R}^{M\times N}$ *whose modulus entries* ϕ_{ij} *are i.i.d. with* $\phi_{ij} \sim \mathrm{SSub}(1/M)$*. Let* $\mathbf{y} = \mathbf{\Phi}\mathbf{x}$ *for any* $\mathbf{x} \in \mathbb{R}^N$*. Then for any* $\epsilon > 0$*,*

$$\mathbb{E}\left(\|\mathbf{y}\|_2^2\right) = \|\mathbf{x}\|_2^2 \tag{A.102}$$

and

$$\mathbb{P}\left(\left|\|\mathbf{y}\|_2^2 - \|\mathbf{x}\|_2^2\right| \geq \epsilon\|\mathbf{x}\|_2^2\right) \leq 2\exp\left(-\frac{M\epsilon^2}{\mu}\right) \tag{A.103}$$

with $\mu = 2/(1-\log(2)) \approx 6.52$*.*

Proof. Let $\phi_{i,:}$ be the i-th row of $\mathbf{\Phi}$. Then i-th entry of $\mathbf{y}$ can be written as $[y]_i = \langle\phi_{i,:}, \mathbf{x}\rangle$, and by applying Lemma 3 we have $Y_i \sim \mathrm{SSub}\left(\|\mathbf{x}\|_2^2/M\right)$. The result follows by using Corollary 1 for $\mathbf{y} = [Y_1, Y_2, \ldots, Y_N]$. □

Lemma 6 ([16, Lemma 7.5])**.** *Let* $\epsilon \in (0,1)$*. There exists a set of points* Q *such that* $|Q| \leq (3/\epsilon)^K$ *and for any* $\mathbf{x} \in \mathbb{R}^K$ *with* $\|\mathbf{x}\|_2 \leq 1$ *there is a point* $\mathbf{q} \in Q$ *which satisfies* $\|\mathbf{x}-\mathbf{q}\|_2 \leq \epsilon$*.*

Proof. We start adding arbitrary $\mathbf{q}_i \in \mathbb{R}^K$ to Q such that $i = 1, 2, \ldots, l$,$\|\mathbf{q}_i\|_2 \leq 1$ and $\|\mathbf{q}_i - \mathbf{q}_j\|_2 > \epsilon$ for all $i > j$ until we can add no more points $(\mathbf{q}_{i>l})$ to Q, where $l = |Q|$. Therefore, for any $\mathbf{x} \in \mathbb{R}^K$ with $\|\mathbf{x}\|_2 \leq 1$ there is a $\mathbf{q} \in Q$ that satisfies $\|\mathbf{x}-\mathbf{q}\|_2 \leq \epsilon$. By centering balls of radius $\epsilon/2$ at each $\mathbf{q}_i$ the balls are disjoint and within a ball of radius $1+\epsilon/2$. If $B^K(r)$ denotes a ball of radius r in $\mathbb{R}^K$, then

$$|Q|\,\mathrm{Vol}\left(B^K(\epsilon/2)\right) \leq \mathrm{Vol}\left(B^K(1+\epsilon/2)\right) \tag{A.104}$$

and therefore

$$|Q| \leq \frac{\mathrm{Vol}\left(B^K\left(1+\epsilon/2\right)\right)}{\mathrm{Vol}\left(B^K\left(\epsilon/2\right)\right)} = \frac{\left(1+\epsilon/2\right)^K}{\left(\epsilon/2\right)^K} \leq \left(3/\epsilon\right)^K. \tag{A.105}$$

□

Now, we are ready to prove Theorem 4.

Proof. Without loosing generality it is enough to prove (2.5) in the case $\|x\|_2 = 1$. We define X_T as s-dimensional subspace of $\mathbf{\Phi}_{[:,T]}$, $T \subset [N]$ and $|T| = s$. We choose finite set of points Q_T such that $Q_T \subseteq X_T$, $\|\mathbf{q}\|_2 \leq 1$ for all $\mathbf{q} \in Q_T$, and for all $\mathbf{x} \in Q_T$ with $\|\mathbf{x}\|_2 \leq 1$ we have

$$\min_{\mathbf{q}\in Q_T} \|\mathbf{x}-\mathbf{q}\|_2 \leq \delta_s/14. \tag{A.106}$$

Here, we have chosen particular value $\delta_s/14$ which makes the proof easier, however, it can be replaced by any smaller arbitrary value. From Lemma 6, we know that $|Q_T| \leq (42/\delta_s)^s$. By collecting all points Q_T with possible sets of T together we obtain:

$$Q = \bigcup_{T:|T|=s} Q_T. \tag{A.107}$$

There are $\binom{N}{s}$ possible index sets T. From stirling's approximation we have $s! \approx \sqrt{2\pi s}\left(\frac{s}{e}\right)^s$, and we have

$$\binom{N}{s} \leq \frac{N^s}{s!} \approx \frac{1}{\sqrt{2\pi s}}\left(\frac{eN}{s}\right)^s < \left(\frac{eN}{s}\right)^s. \tag{A.108}$$

Therefore,

$$|Q| \leq \left(42eN/\delta_s s\right)^s. \tag{A.109}$$

From Corollary 1 we have (A.101). Hence

$$\mathbb{P}\left(\left|\| \mathbf{\Phi}\mathbf{q} \|_2^2 - \| \mathbf{q} \|_2^2\right| \geq \epsilon \| \mathbf{q} \|_2^2\right) \leq 2\exp\left(-\frac{M\epsilon^2}{\mu}\right), \quad \text{for all}\, \mathbf{q} \in Q_T. \tag{A.110}$$

By applying (A.109) we obtain

$$\mathbb{P}\left(\left|\| \mathbf{\Phi}\mathbf{q} \|_2^2 - \| \mathbf{q} \|_2^2\right| \geq \epsilon \| \mathbf{q} \|_2^2\right) \leq 2\left(\frac{42eN}{\delta_s s}\right)^s \exp\left(-\frac{M\epsilon^2}{\mu}\right), \text{for all}\;\; \mathbf{q} \in Q \tag{A.111}$$

$$\mathbb{P}\left(\left|\| \mathbf{\Phi}\mathbf{q} \|_2^2 - \| \mathbf{q} \|_2^2\right| \leq \epsilon \| \mathbf{q} \|_2^2\right) > 1-2\left(\frac{42eN}{\delta_s s}\right)^s \exp\left(-\frac{M\epsilon^2}{\mu}\right), \text{for all}\;\; \mathbf{q} \in Q. \tag{A.112}$$

Setting $\epsilon = \delta_s/\sqrt{2}$ in (A.112) gives

$$\left(1 - \delta_s/\sqrt{2}\right) \|\mathbf{q}\|_2^2 \leq \|\mathbf{\Phi q}\|_2^2 \leq \left(1 + \delta_s/\sqrt{2}\right) \|\mathbf{q}\|_2^2\,, \ \text{for all}\, \mathbf{q} \in Q \tag{A.113}$$

with probability greater than

$$1 - 2\left(42eN/\delta_s s\right)^s e^{-M\delta_s^2/2\mu}. \tag{A.114}$$

We observe that if M satisfies (2.10) then

$$\log\left(\frac{42eN}{\delta_s s}\right)^s \leq s\log\left(\frac{N}{s}\right)\log\left(\frac{42e}{\delta_s}\right) \leq \frac{M\log\left(42e/\delta_s\right)}{\alpha} \tag{A.115}$$

and (A.114) will change to $1 - 2e^{-\beta M}$ as desired.
Now we define θ as the smallest number such that

$$\|\mathbf{\Phi x}\|_2 \leq \sqrt{1+\theta}\, \|\mathbf{x}\|_2 \ \text{ for all } x \in X_T,\ \|\mathbf{x}\|_2 \leq 1. \tag{A.116}$$

If we show that $\theta \leq \delta_s$ then the proof is completed. We pick $\mathbf{q} \in Q_T \subset X_T$ and for any $\mathbf{x} \in X_T$ we have $\|\mathbf{x} - \mathbf{q}\|_2 \leq \delta_s/14$. From (A.113) and (A.116) we have that

$$\|\mathbf{\Phi x}\|_2 \leq \|\mathbf{\Phi q}\|_2 + \|\mathbf{\Phi}(\mathbf{x} - \mathbf{q})\|_2 \leq \sqrt{1 + \delta_s/\sqrt{2}} + \delta_s/14\sqrt{1+\theta}. \tag{A.117}$$

By definition θ is the smallest number for which (A.116) holds, therefore,

$$\sqrt{1+\theta} \leq \sqrt{1 + \delta_s/\sqrt{2}} + \delta_s/14\sqrt{1+\theta} \tag{A.118}$$

and

$$\sqrt{1+\theta} \leq \frac{\sqrt{1 + \delta_s/\sqrt{2}}}{1 - \delta_s/14} \leq \sqrt{1+\delta_s}. \tag{A.119}$$

We have proved the upper inequality in (2.5). Similarly, for lower bound we have

$$\|\mathbf{\Phi x}\|_2 \geq \|\mathbf{\Phi q}\|_2 - \|\mathbf{\Phi}(\mathbf{q} - \mathbf{x})\|_2 \geq \sqrt{1 - \delta_s/\sqrt{2}} - \delta_s/14\sqrt{1-\theta} \geq \sqrt{1-\delta_s}, \tag{A.120}$$

which completes the proof. $\square$

Appendix B

A model for the measurement noise in 1-bit compressive sensing

In the case that there is measurement noise we have

$$\operatorname{sign}\left(\Phi\mathbf{x}+\mathbf{n}\right)=\tilde{\mathbf{b}}_m, \tag{B.1}$$

where $\mathbf{n}\in\mathbb{R}^M$ is the measurement noise and $[\mathbf{n}]_i\sim\mathcal{N}\left(0,\sigma_n^2\right)$ for all i. First, we find the distribution of $[\Phi\mathbf{x}]_i$. Each element of $\Phi\mathbf{x}$ is the summation of s multiplication pairs of $\phi_{i,j}\sim N\left(0,\sigma_\phi^2\right)$ and $[\mathbf{x}]_j\sim\mathcal{N}\left(0,\sigma_x^2\right)$. In [26, section 6.A], the distribution of multiplication of two independent s dimension Gaussian vectors has been calculated. Recall that s is the sparsity of $\mathbf{x}$, $\sigma_x^2=1$ and $\sigma_\phi^2=1/M$ where M is the number of rows in Φ. We are looking for the probability of the bit flip in each bit of $\tilde{\mathbf{b}}_m$ which is denoted by P_{fm}. Therefore,

$$P_{fm}=\mathbb{P}\left(\operatorname{sign}\left([\Phi\mathbf{x}+\mathbf{n}]_i\right)\neq\operatorname{sign}\left([\Phi\mathbf{x}]_i\right)\right). \tag{B.2}$$

We assume that $[\mathbf{n}]_i=n$, $[\Phi\mathbf{x}]_i=\theta$ and $\theta>0$ then we have

$$\begin{aligned}P_{fm} &= 2\int_0^\infty p_N\left(n<-\theta\right)p_\Theta\left(\theta\right)d\theta\\ &= 2\int_0^\infty\left(1-Q\left(\frac{\theta}{\sigma_n^2}\right)\right)p_\Theta\left(\theta\right)d\theta,\end{aligned} \tag{B.3}$$

where $p_\Theta\left(\theta\right)$ is shown in [26, section 6.A]. Intuitively, when $\sigma_n^2=0$, $P_{fm}=0$ and as σ_n^2 tends to infinity P_{fm} converges to $\frac{1}{2}$.

Bibliography

[1] A. Jerri, "The shannon sampling theorem-its various extensions and applications: A tutorial review," *Proceedings of the IEEE*, vol. 65, no. 11, pp. 1565–1596, 1977.

[2] E. Candès, "Compressive sampling," in *Proceedings on the International Congress of Mathematicians*, Madrid, Spain, Aug. 2006, pp. 1433–1452, invited lectures.

[3] R. Baraniuk, "Compressive sensing [lecture notes]," *Signal Processing Magazine, IEEE*, vol. 24, no. 4, pp. 118–121, 2007.

[4] E. Candès and M. Wakin, "An introduction to compressive sampling," *Signal Processing Magazine, IEEE*, vol. 25, no. 2, pp. 21–30, 2008.

[5] E. Candès and T. Tao, "Decoding by linear programming," *IEEE Transactions on Information Theory*, vol. 51, no. 12, pp. 4203–4215, 2005.

[6] J. Tropp and S. Wright, "Computational methods for sparse solution of linear inverse problems," *Proceedings of the IEEE*, vol. 98, no. 6, pp. 948–958, 2010.

[7] J. Laska and R. Baraniuk, "Regime change: Bit-depth versus measurement-rate in compressive sensing," *Arxiv preprint arXiv:1110.3450*, 2011.

[8] P. Boufounos and R. Baraniuk, "1-bit compressive sensing," in *42nd Annual Conference on Information Sciences and Systems (CISS)*, Mar. 2008, pp. 16–21.

[9] L. Jacques, J. Laska, P. Boufounos, and R. Baraniuk, "Robust 1-bit compressive sensing via binary stable embeddings of sparse vectors," *Arxiv preprint arXiv:1104.3160*, 2011.

[10] M. Yan, Y. Yang, and S. Osher, "Robust 1-bit compressive sensing using adaptive outlier pursuit," *IEEE Transactions on Signal Processing*, vol. 2, p. 3, 2012.

[11] B. Natarajan, "Sparse approximate solutions to linear systems," *SIAM Journal on Computing*, vol. 24, no. 2, pp. 227–234, 1995.

[12] H. Rauhut, "Compressive sensing and structured random matrices," *Theoretical Foundations and Numerical Methods for Sparse Recovery*, vol. 9, pp. 1–92, 2010.

[13] A. Tulino and S. Verdú, *Random matrix theory and wireless communications.* Now Publishers Inc, 2004, vol. 1.

[14] E. Candès, "An introduction to compressed sensing," Isaac Newton Institute, LMS - Invited Lecturer Series, 2011.

[15] V. Buldygin and I. Kozachenko, *Metric characterization of random variables and random processes.* American Mathematical Society, 2000.

[16] R. Baraniuk, M. Davenport, M. Duarte, and C. Hegde, "An Introduction to Compressive Sensing," *http://cnx.org/content/col11133/1.5/*, April 2, 2011.

[17] T. Blumensath and M. Davies, "Iterative hard thresholding for compressed sensing," *Applied and Computational Harmonic Analysis*, vol. 27, no. 3, pp. 265–274, 2009.

[18] D. Needell and J. Tropp, "Cosamp: Iterative signal recovery from incomplete and inaccurate samples," *Applied and Computational Harmonic Analysis*, vol. 26, no. 3, pp. 301–321, 2009.

[19] Y. Plan and R. Vershynin, "One-bit compressed sensing by linear programming," *Arxiv preprint arXiv:1109.4299*, 2011.

[20] P. Boufounos, "Greedy sparse signal reconstruction from sign measurements," in *Conference Record of the Forty-Third Asilomar Conference on Signals, Systems and Computers.* IEEE, 2009, pp. 1305–1309.

[21] M. Shetty, *Nonlinear programming.* Wiley Online Library, 1993.

[22] R. Horn and C. Johnson, *Matrix analysis.* Cambridge university press, 2005.

[23] E. Coddington, *An introduction to ordinary differential equations.* Dover Pubns, 1989.

[24] R. Adler, “An introduction to continuity, extrema, and related topics for general Gaussian processes,” *Lecture Notes-Monograph Series*, vol. 12, 1990.

[25] R. Vershynin, “Introduction to the non-asymptotic analysis of random matrices,” *Arxiv preprint arxiv:1011.3027*, 2010.

[26] M. Simon, *Probability distributions involving Gaussian random variables: A handbook for engineers and scientists.* Springer Verlag, 2006.